Biostratigraphy and chemostratigraphy of the lower Cambrian Normanville Group, South Australia

Ciaran Philip Mathewson

Masters of Research (MRes)

Supervisor: Assoc. Prof. Glenn A. Brock

Department of Biological Sciences

Macquarie University, Sydney, Australia

Sample location at Southern Quarries, Sellicks Hill, South Australia. C.P. Mathewson (2016).

Submitted on 10 October, 2016

Table of Contents

Abstract

Australia has lagged behind in constructing a workable lower Cambrian regional biostratigraphic scheme. However, recent work utilising both bio- and chemostratigraphic data has produced a robust chronostratigraphic scheme for the Arrowie Basin in South Australia. This multi-proxy approach provides independent datasets that facilitate refined chronostratigraphic correlation of Australian lower Cambrian rock packages with the global Cambrian timescale. The *Kulparina rostrata* Zone in the Arrowie Basin closely aligns with a significant **negative** $\delta^{13}C$ (carbon-13/12 isotope ratio) excursion, the 'SHICE'. A key prediction of this correlation was that older successions in the neighbouring Stansbury Basin should contain a significant **positive** $\delta^{13}C$ isotope excursion, the 'ZHUCE'.

This study, using similar multi-proxy data for the eastern Stansbury Basin, tested the validity of this prediction. The topmost 83 m of the 'WANG' section was confidently correlated with the *Kulparina rostrata* Zone based on co-occurring, diagnostic fossil assemblages. The chemostratigraphic results closely match the global chemostratigraphic curve. The 'SHICE' negative excursion occurs within the upper Sellick Hill Formation. Significantly, a large positive $\delta^{13}C$ excursion (max +5.70‰) was discovered in the lower Sellick Hill Formation; interpreted to represent the global 'ZHUCE' positive $\delta^{13}C$ event which is identified from Australia for the first time, confirming previous chronostratigraphic predictions.

Declaration

The body of this thesis follows the format for a manuscript submission to the international peer-review journal *Geological Magazine* [ISSN: 0016-7568], using the journal instructions accessed at http://assets.cambridge.org/GEO/GEO_ifc.pdf.

All research was conducted with funding from Macquarie University HDR Funds and research funds from Assoc. Prof. Glenn A. Brock of Macquarie University.

I would like to acknowledge the following for assistance in this thesis:

Assoc. Prof. Glenn A. Brock from the Macquarie University Palaeobiology Lab for stubbing the microfossil specimens for SEM examination.

Dr. Sarah Jacquet from the Macquarie University Palaeobiology Lab for polishing the lithological blocks so they could be photographed and for the preliminary designs of the stratigraphic columns.

Mark Rollog from the University of Adelaide for performing the data corrections on the carbon and oxygen isotopic analyses.

The isotopic data of the SHL, MORO, BHG and WAR sections were collected by Dr. Marissa Betts from the Macquarie University Palaeobiology Lab for her PhD (Fossils, rocks and Cambrian clocks: A multi-proxy approach to chronologically subdividing the lower Cambrian of the Arrowie Basin, South Australia, 2016) at Macquarie University. All interpretations of this data are my own work.

No Ethics Committee approval was necessary for this research.

I hereby certify that this thesis is my own work and has not been submitted for a Higher Degree at any other University or Institution.

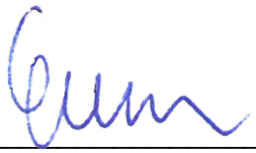

CIARAN PHILIP MATHEWSON

10 OCTOBER, 2016

Acknowledgements

Firstly, I would like to give a huge thank you to my Supervisor Assoc. Prof. Glenn Brock, without whom I wouldn't have decided on this undertaking in the first place. His experience and deep knowledge of palaeobiology has taught me an enormous amount, not to mention his ability to always have an answer on hand if ever I asked, as well as providing any extra funding that was necessary. I hope our rapport will continue for years to come.

To Dr. Marissa Betts, the predictions from your PhD thesis are what allowed me to pursue this particular topic, as well as your sharing with me the unpublished isotopic data from the Arrowie and Stansbury Basins for use in this research. Thank you also for your substantial help in the acid room, on the rock saw, puzzling out how to correctly drill out samples and your incredibly efficient tips on the SEM made my life so much easier. To Dr. Sarah Jacquet, I would have been lost without your knowledge of Adobe Photoshop and Illustrator, which made the creation (and considerable editing) of figures almost simple to do. Also, my stratigraphic column would be an absolute mess without your input, and thank you for helping to sand down my polished blocks to a clearly useable level. To both of you, many thanks, I will fondly remember our lunchtime conversations that were both meaningful and sometimes downright insane.

A big thank you to the other Macquarie University staff: David Mathieson in the Palaeobiology Lab for induction to the Acid Leaching Facility and endless tips on how to keep fragmentation to a minimum; Dr. Matthew Kosnik for excellent ideas on simple yet effective presentations and the use of the Dremel; Manal Bebbington from EPS for her help with all my early mornings at the rock saw (and changing of saw blades); and Sue Lindsay from the MQU Microscopy Unit for inducting me in use of the SEM, gold-coating of my specimens and overseeing to make sure I didn't break anything.

I must acknowledge my friends and colleagues from Adelaide, without whom all my research would have been for nothing. Tom and Sandra Bradley, thank you so much for letting me stay at your home during my fieldwork, our conversations (and limericks) were second to none, as were the peaches direct from your tree and your generous hospitality. A second thank you to Tom for helping to collect samples in the quarry.

To Trevor Smith at Southern Quarries Ltd., for giving permission to gather samples in the quarry and organising access and sampling of the section on a weekend, outside of regular quarry operating hours. Prof. Jim Jago and Nick Langsford from the University of South Australia, thank you for your help in identifying formation boundaries in the field and sample collection. Thank you

also to Dr. Wolfgang Preiss of the Geological Survey of South Australia for help collecting samples within the quarry.

From the University of Adelaide, thank you to Dr. Diego Garcia-Bellido for sample collection and transport to and from the sample site, as well as the use of the camera drone which gave fantastic video and images of the quarry site. A huge thank you to Mark Rollog for inducting me into the mysteries of the mass spectrometer, showing me how to properly retrieve the isotope data, and dealing with the very fickle electronics of the machine, as well as performing the data corrections for the isotope sample data.

Finally, to my family and friends who have supported this endeavour, my ability to explain the subject matter in simple terms has improved immeasurably, and it truly did help for presentations throughout this unit. I hope your interest in palaeontological matters increases, even if only slightly, from listening to my lectures on the topic.

1. Introduction

The Cambrian period is the oldest in the Phanerozoic Eon, beginning ~541 million years ago, and represents the primary interval of the initial major radiation of bilaterian animal life – those animals which dominate all ecosystems on Earth today (Marshall 2006, Erwin *et al.* 2011, Erwin & Valentine 2012). The Cambrian radiation set the stage for modern biodiversity, trophic structure and ecological networks. This extraordinary burst of evolutionary diversification resulted in the emergence of a wide range of animal body plans and is recognised as the origin of most modern animal phyla.

Subdivision of the geological timescale, especially during the Cambrian period, is vital to enable the chronological organisation, interpretation and correlation of the key evolutionary, ecological and geological events on a global scale. In 2004, the International Subcommission on Cambrian Stratigraphy (ISCS) split the Cambrian period into four 'series', which were further subdivided into ten 'stages', each of approximately equal length (Fig. 1). The lower boundary of each stage is defined (or proposed to be defined) by the First Appearance Datum (FAD) of key fauna associated with diversification and evolutionary events. Boundaries ultimately are identified by GSSPs (Global Boundary Stratotype Section and Point) after rigorous study and reliable multi-

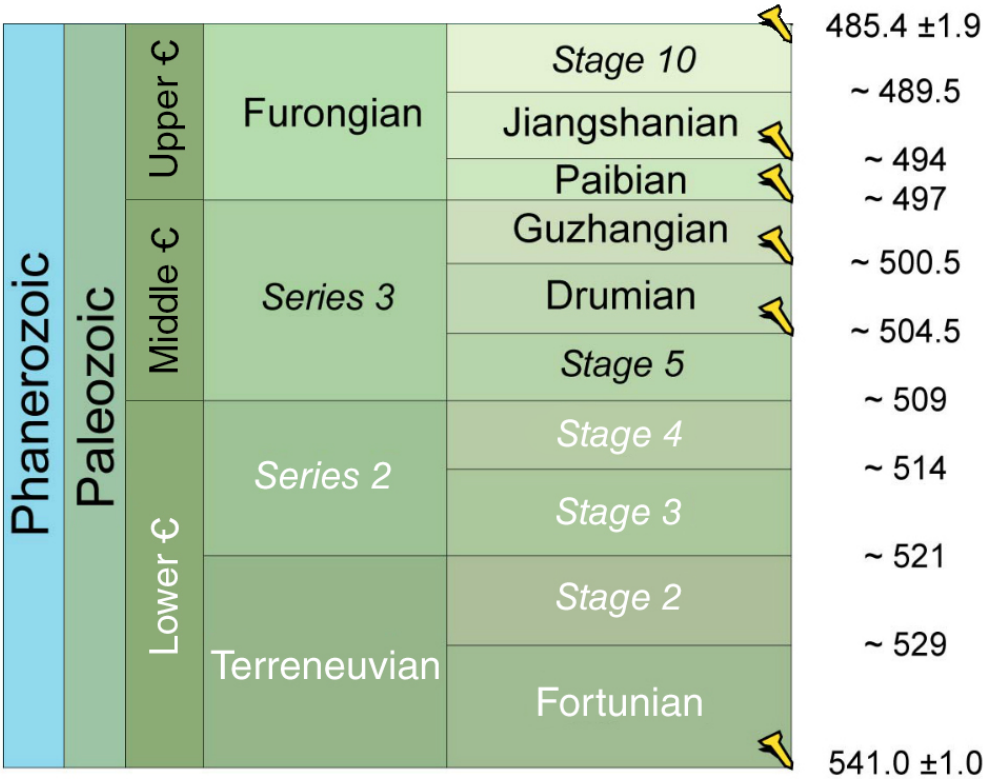

Figure 1. The Series and Stage subdivision of the Cambrian (Є) period. Yellow nails indicate GSSPs. Lower Cambrian period highlighted in white. Italicised Series 2 and 3, and Stages 2-5 remain undefined. Modified from The International Chronostratigraphic Chart v2016 at www.stratigraphy.org.

proxy evidence before they are formally named and defined (Babcock *et al.* 2005, Babcock & Peng 2007, Peng & Babcock 2011, Peng *et al.* 2012*a, b*). For example, the lower boundary of the Furongian Series and the conterminant Paibian Stage (Fig. 1) aligns with the FAD of the cosmopolitan agnostid species *Glyptagnostus reticulatus*, as well as the globally recognised Steptoean Positive Carbon Isotopic Excursion (SPICE; Peng *et al.* 2004; Saltzman *et al.* 2000, 2004). Trilobites and agnostid arthropods are particularly well-studied fossil groups and are effective as index fossils for the biostratigraphical subdivision of Cambrian Stage 3 and younger intervals. They are very well-preserved, relatively easy to identify and contain many cosmopolitan species with short stratigraphic ranges (Babcock *et al.* 2005, 2007; Peng *et al.* 2004, 2012*b*; Zhu *et al.* 2004). Trilobites and agnostid arthropods are index fossils for defining the bases of Stages 5 through 10 (Babcock *et al.* 2007; Babcock & Peng 2007; Peng *et al.* 2009, 2012*a, b*).

Whilst Series 3 and Furongian rocks are the best defined in the Cambrian period (Fig. 1), global correlation using the older series is still developing and separate regions with Cambrian rocks (representing separate palaeocontinents) rely on different fossils, often endemic, to identify their own regional biostratigraphic schemes (Peng *et al.* 2012*a, b*; Betts *et al.* 2016). The traditional lower Cambrian period is subdivided (in ascending stratigraphic order) into the Terreneuvian Series and unnamed Series 2. The Terreneuvian Series is subdivided into two stages: the lowermost Fortunian Stage, succeeded by unnamed Stage 2. Cambrian Series 2 is subdivided into the unnamed and undefined Stages 3 and 4. The lack of trilobites in pre-Series 2 strata (Fortunian to Stage 2) has meant that correlation for these packages relies heavily on the detailed description of non-trilobite fossil groups and until very recently Australia has lagged behind in constructing a workable lower Cambrian regional biostratigraphic scheme (Fig. 2). As such, the lower Cambrian pre-Series 2 is the mostly poorly defined time interval within the Cambrian period.

In Australia, key fossil groups useful in subdividing Fortunian to Stage 2 aged deposits include: sponge-like archaeocyathids (Debrenne & Gravestock 1990, Zhuravlev & Gravestock 1994, summary in Brock *et al.* 2000) represented by three assemblage zones around the Terreneuvian Series, Stage 2 – Series 2, Stage 3 boundary; acritarchs of which seven assemblage zones have been identified throughout the lower Cambrian period (Zang *et al.* 2007, Jago *et al.* 2012); and a range of stem-group lophotrochozoan, biomineralised animals which were previously lumped together under the umbrella term ‘small shelly fossils’, or SSFs (Matthews & Missarzhevsky 1975; Steiner *et al.* 2004, 2007; Skovsted *et al.* 2006; Betts *et al.* 2014; Devaere *et al.* 2013, 2014). Detailed SSF research over the last decade has highlighted the biostratigraphic utility of many SSF taxa, including detailed interpretations of complete body plans of creatures that

were only previously known from isolated skeletal components (e.g. Topper *et al.* 2013; Skovsted *et al.* 2008, 2009, 2015; Larsson *et al.* 2014).

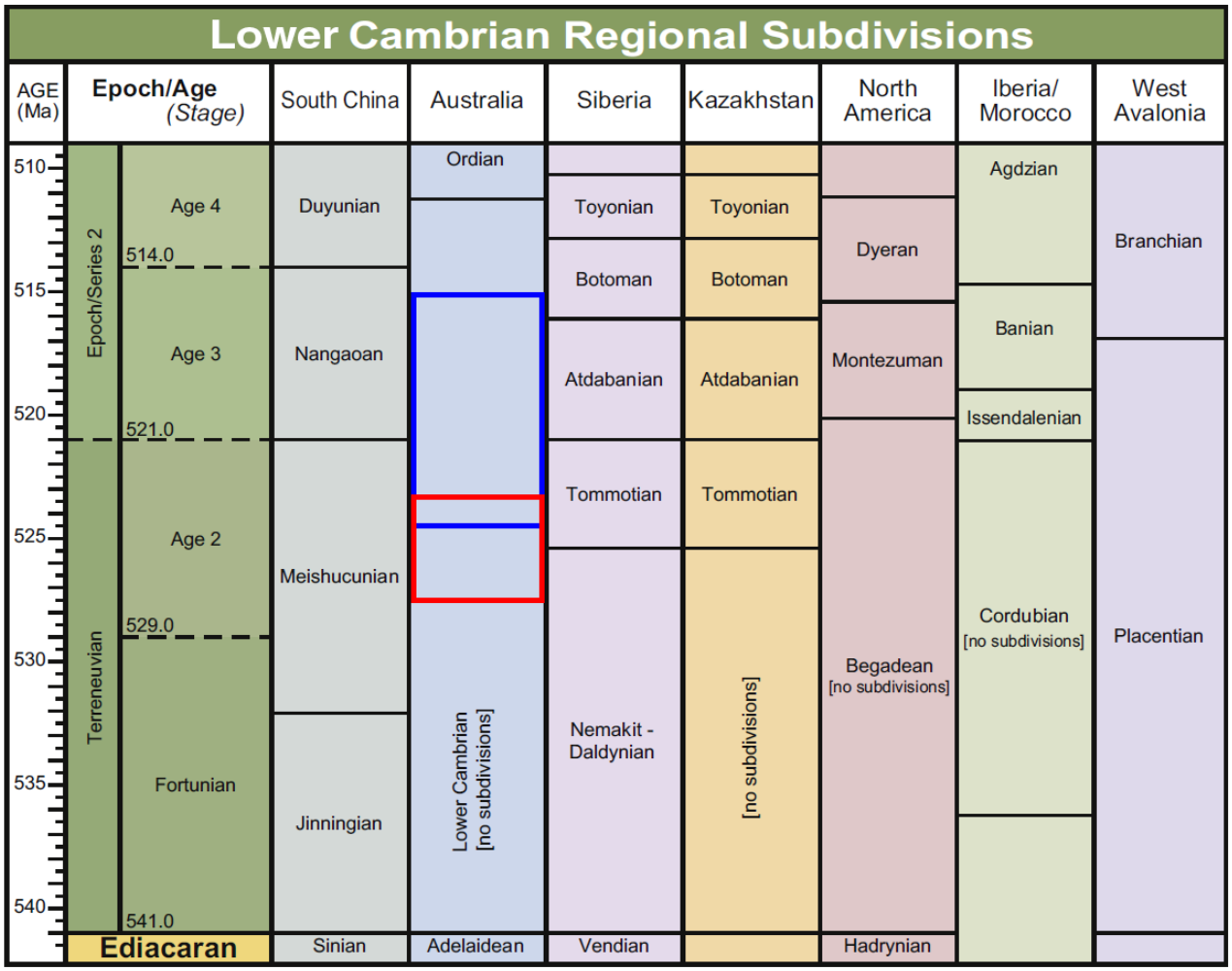

Figure 2. Lower Cambrian subdivisions separated into global regions. Note the lack of subdivisions in Australia. Red box = time interval of this study. Blue box = time interval from Betts *et al.* (2016). Modified from Peng *et al.* (2012*a*).

Formal ratification of lower Cambrian stages is lacking, largely as a result of high levels of endemism and facies restricted distribution in archaeocyathids and SSFs (Landing & Geyer 2012, Landing *et al.* 2013), as well as taphonomic and taxonomic difficulties in dealing with acritarchs hindering global correlation. All biostratigraphic schemes (especially global) must be tested rigorously across separate palaeocontinents to ensure accurate chronostratigraphy. For example, the micromollusc *Watsonella crosbyi* Grabau (1900), has a near-cosmopolitan distribution, with first occurrence data known from China, France, Mongolia, Avalonia, Siberia and Australia that suggests great global potential for correlation (Brasier *et al.* 1996, Li *et al.* 2011, Kouchinsky *et al.* 2012, Devaere *et al.* 2013, Jacquet *et al.* in press). Consequently, the taxon has been suggested as the best index fossil to define the lower boundary Cambrian Stage 2 (Li *et al.* 2011, Parkhaev & Karlova 2011, Peng & Babcock 2011, Peng *et al.* 2012*b*, Landing & Kouchinsky 2016). This contribution focusses on the biostratigraphy of SSFs, which Betts *et al.* (2016) have demonstrated

can provide robust and repeatable regional biostratigraphic schemes with potential for global correlation. Though some endemism and facies restriction of taxa is inevitable (Landing & Geyer 2012, Landing *et al.* 2013), the fact remains that many shelly fossils (e.g. halkieriids, palaeoscolecids, hyoliths, brachiopods) occur in a much wider range of facies than do archaeocyaths and acritarchs and thus have more potential for correlation. Whilst there are clearly difficulties in global correlation using Cambrian fossils, there is still a remarkable amount of precision and robustness in regional-scale biostratigraphy (e.g. Rozanov *et al.* 1969, Missarzhevsky & Mambetov 1981, Brasier *et al.* 1996, Steiner *et al.* 2007, Devaere *et al.* 2013, Betts *et al.* 2016). Further, the global difficulties can be minimised when regional biostratigraphic schemes are used in concert with independent correlative tools such as chemostratigraphy.

1.a. Chemostratigraphy – context and background

Chemostratigraphy is the study of the chemical variance of fossilized shells and bulk rock samples from stratigraphic successions through time. Carbon-isotope chemostratigraphy is directly affected by major biological transitions, as plants and animals are critical drivers of the carbon cycle (Maloof *et al.* 2010*a*). Inorganic carbon-isotope chemostratigraphy is essentially founded on measuring the ratio between two isotopes: ^{12}C and ^{13}C. The lighter ^{12}C isotope is preferentially utilised by primary producers in cellular activities, hence it becomes depleted in the hydrosphere and atmosphere. Further, it means that in times of high primary productivity, more ^{12}C is sequestered by organisms, leaving less to be locked up within the carbonate sediments laid down in that period, therefore increasing the inorganic $^{13}C/^{12}C$ ratio. Brasier (1993) described this process as well as the potential of chemostratigraphy as a correlative method – isotopic changes spread globally within a short temporal period, thus any change should be reflected globally. This change in the carbon-isotope ratio through a stratigraphic package of rocks, expressed as $\delta^{13}C$, is represented as a curve fluctuating around a zero per mill (‰) level, becoming either positive (more ^{13}C) or negative (more ^{12}C) as measured in whole rock or calcareous shelly fossil samples (Saltzman & Thomas 2012). Any large positive or negative swings are known as excursions, and these perturbations, as with defining biostratigraphic divisions, may be associated with key oceanic, geochemical and ultimately evolutionary events related to faunal turnover and extinction.

Carbon-isotope chemostratigraphy is recognised as an effective correlation tool within the Early Cambrian period because it is relatively robust, largely independent of facies and an important independent chronostratigraphic tool that can constrain endemic faunas and regional biostratigraphic schemes, especially in pre-trilobitic lower Cambrian packages. As an independent

technique, chemostratigraphy can undoubtedly be very effective (e.g. Maloof *et al.* 2010*a*, *b*; Kouchinsky *et al.* 2012, Landing *et al.* 2013) although it is important that sources of potential diagenesis, such as sub-aerial exposure, shell recrystallization, organic burial rates, the presence of hardgrounds and local depositional conditions such as exposure to contaminated groundwater are identified and addressed (Kaufmann & Knoll 1995, Wendler 2013, Bradbury *et al.* 2015, Miall 2015, Swart 2015). Since carbonates hold a record of both carbon and oxygen, the oxygen-isotope curves can also be determined and plotted along with the $\delta^{13}C$ data. Oxygen-isotope chemostratigraphy (based on the $^{18}O/^{16}O$ ratio) has both the benefit and the detriment of being more strongly affected by temperature and diagenesis than carbon isotopes. This volatility allows oxygen isotopes to be used for measurements of palaeotemperature and palaeoclimate (e.g. Fricke *et al.* 1998, Clarke & Jenkyns 1999, Johnsen *et al.* 2001, Weissert & Erba 2004).

Unfortunately this also means that rocks which have undergone strong diagenesis will show uncharacteristic oxygen-isotope values, but when used alongside the less volatile carbon-isotope values, oxygen-isotope values can be used to reveal these diagenetic changes. The general trend in rocks exhibiting diagenetic change is for the $\delta^{18}O$ values to positively spike, whilst the $\delta^{13}C$ values become more negative (Melim *et al.* 2001). Thus, if the carbon and oxygen curves independently exhibit uncharacteristic spikes within the same horizon, it can indicate likely diagenesis within samples. Geological isotopic composition from carbonates should ideally come from calcareous shell material itself, giving a direct signal as the shell is laid down in equilibrium with surrounding water chemistry (Weissert *et al.* 2008). However, calcareous shells are not common in lower Cambrian successions and so bulk rock samples collected from cut carbonate blocks provide the best means for determining isotopic compositions. As long as sample preparation protocols are followed to limit the possibility of sampling *ex situ* material, the robust nature of isotopic data will often reveal signals and trends of $\delta^{13}C$ and $\delta^{18}O$ data that correspond to true global signals. The production of a robust chemostratigraphic curve provides an independent method that can be used alongside a robust regional biostratigraphic scheme to refine and calibrate each other as part of a multi-proxy approach to chronostratigraphy.

The ‘wiggle-matching’ concept to align the positive and negative peaks of chemostratigraphic correlation (Weissert *et al.* 2008) is only effective during periods of rapid, major changes in isotopic ratios so, in this regard, the Cambrian period is ideal for chemostratigraphic methods (Fig. 3). Within lower Cambrian Stage 2, the most important carbon-isotope excursion events include the ZHUCE (Zhujiaqing Carbon-Isotope Excursion) and slightly younger SHICE (Shiyantou Carbon-Isotope Excursion). The base of the succeeding Cambrian Stage 3 is characterised by the presence of the CARE (Cambrian Arthropod Radiation Isotope Excursion).

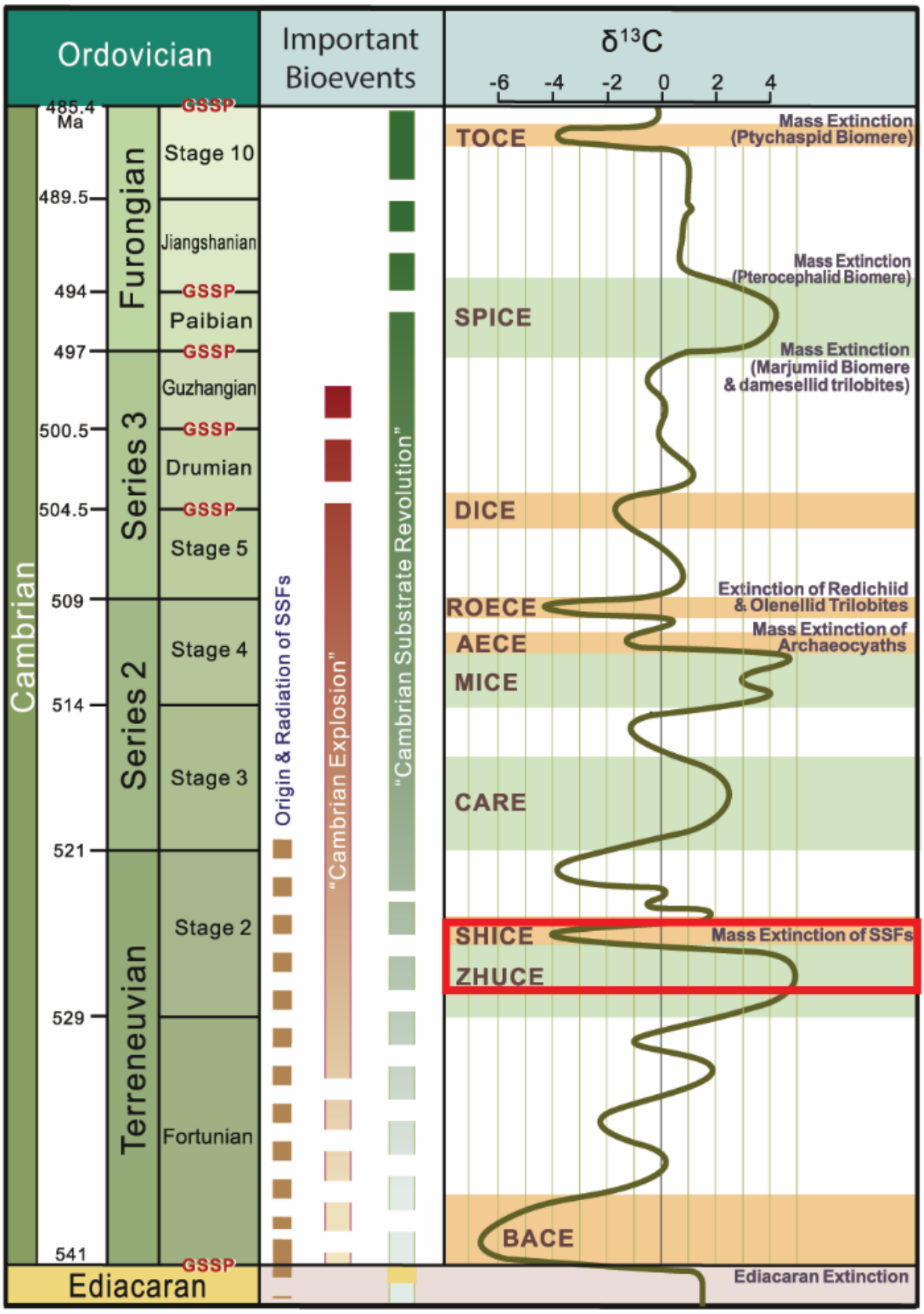

Figure 3. The global chemostratigraphic curve of the Cambrian period, showing key positive (shaded green) and negative (shaded orange) excursions. The time interval covered by this study is boxed in red. Modified from Peng *et al.* (2012*a*).

The ZHUCE $\delta^{13}C$ event aligns with a major radiation of SSFs (Zhu *et al.* 2006, Landing & Kouchinsky 2016) and is one of the largest positive excursions within the lower Cambrian period, coinciding with the rise of the first mineralised metazoans. The SHICE $\delta^{13}C$ event is a negative excursion corresponding to a major extinction of small shelly fossils located at the eponymous Shiyantou Formation in China and the CARE $\delta^{13}C$ event is a positive excursion corresponding to the first major radiation of arthropods (especially trilobites) on a global scale (Zhu *et al.* 2006). Each of these major excursions contain multiple minor 'peaks' throughout the excursion period, making peak-matching using chemostratigraphy alone fraught with difficulty. However, when calibrated with well-constrained and robust regional biostratigraphic schemes, constraining isotopic curves becomes increasingly more accurate and highly resolved.

1.b. The Zhujiaqing Carbon-Isotope Excursion (ZHUCE)

The ZHUCE $\delta^{13}C$ event was originally identified on the Yangtze Platform in South China (Zhu *et al.* 2006) and follows a major radiation of the first mineralised organisms within the Cambrian period, including SSFs. The ZHUCE $\delta^{13}C$ event is characterised by the highest positive $\delta^{13}C$ values within the whole Cambrian period and has been recorded in multiple localities across the globe, including China (up to 7‰, Zhou *et al.* 1997, Li *et al.* 2009), Morocco (6-7‰, Maloof *et al.* 2005), Siberia (6‰, Kouchinsky *et al.* 2001) and India (up to 6‰, Aharon *et al.* 1987, Knoll *et al.* 1995). The peak aligns with positive excursions L4 (China; Li *et al.* 2009) and I' (Siberia; Kouchinsky *et al.* 2001). The excursion begins just after the transition between the undefined Fortunian - Cambrian Stage 2 boundary and close to the Siberian Nemakit-Daldynian - Tommotian boundary (Fan *et al.* 2011) and because of this it has become increasingly significant in recent years. Recently, Landing & Kouchinsky (2016) have suggested that the lower boundary of Cambrian Stage 2 might be defined globally based on the FAD of the geographically widespread micromolluscs *W. crosbyi* and *Aldanella attleborensis*, and the *Skiagia ornata-Fimbrioglomerella membranacea* acritarch 'zone' which occurs below the maximum extent of the ZHUCE $\delta^{13}C$ positive peak (Li *et al.* 2011). If the ZHUCE $\delta^{13}C$ positive could be identified within the Normanville Group of South Australia where the biostratigraphic range of *W. crosbyi* has recently been clarified (see Jacquet *et al.* in press) the prospect of defining the potential lower boundary for Cambrian Stage 2 in Australia would be greatly enhanced.

1.c. A multi-proxy approach to chronostratigraphy

As noted above, chemostratigraphy on its own must be used with caution, but when used alongside other independent time constrained data, such as biostratigraphic regional schemes, chemostratigraphy provides a much more robust examination of the timescale that can produce reliable results. An exemplar of this multi-proxy methodology is the decade-long chronostratigraphic research focussed on systematic sampling of SSFs from 21 stratigraphic sections from the Hawker Group rocks of the Arrowie Basin, South Australia by Betts *et al.* (2015, 2016) which recently culminated in a new biostratigraphic scheme for the lower Cambrian period of South Australia (Betts *et al.* 2015, 2016, in review). Three new biozones were erected based on detailed SSF range data, in ascending order: the *K. rostrata* Zone, *M. etheridgei* Zone and *D. odyssei* Zone, spanning an interval from the upper part of pre-trilobitic Cambrian Stage 2 through to Cambrian Stages 3 and 4. Chemostratigraphic data was also collected from 10 of these sections (Betts *et al.* in prep.) that yielded SSFs and this facilitated direct correlation of the new biozones to the global carbon-isotope chemostratigraphic scheme (see Brasier 1993, Maloof 2010*a*, Ishikawa *et al.* 2014). Betts *et al.* (2016) revealed that the upper part of the *Micrina etheridgei* Zone correlated with the CARE $\delta^{13}C$ positive event across the basin and indicated that the incoming of trilobites in Australia was much closer to the base of Cambrian Stage 3 than previously thought. Betts *et al.* (2016; in review) also found a distinct negative trend in the underlying upper *K. rostrata* Zone which they interpreted as the early stages of the SHICE $\delta^{13}C$ negative.

The new biostratigraphic and chemostratigraphic data from lower Cambrian carbonates in the Arrowie Basin provides testable predictions regarding the chronostratigraphic age and position of carbonate packages of the Normanville Group in the eastern Stansbury Basin. The lack of carbonate lithologies in the Arrowie Basin below the Wilkawillina Limestone and Woodendinna Dolostone preclude further sampling for isotopic data. However, Betts *et al.* (in prep.) predicted that the major peak of the SHICE $\delta^{13}C$ negative event as well as the underlying ZHUCE $\delta^{13}C$ positive should be captured within the lower Cambrian carbonate successions of the Normanville Group (Fig. 4). Jacquet *et al.* (in press) have revealed the lower units of the group lie within Cambrian Stage 2, based on the range of the globally significant molluscan taxon *W. crosbyi*. Adding further support to a Cambrian Stage 2 age is the incoming of the globally distributed tommotiid *Sunnaginia imbricata* above the range of *W. crosbyi* within the Normanville Group (Skovsted *et al.* 2015, Jacquet *et al.* in prep.). Faunal data should provide a means of accurate correlation between the Arrowie and Stansbury Basins, alongside the first chemostratigraphic data of the area which would also facilitate and enhance global correlation. The lower Cambrian rocks of the eastern Stansbury Basin are therefore the focus for this study in order to test the predictions of Betts *et al*. (in prep.).

1.d. Project aims

1. To use biostratigraphic and chemostratigraphic proxy data to resolve the age of the lower Cambrian Normanville Group.

2. To determine whether the ZHUCE/L4/I' global positive carbon isotope excursion occurs in the lower Normanville Group as predicted by previous work.

3. To determine whether the lower boundary of Terreneuvian Series, Stage 2 of the International Cambrian timescale can be identified in the Normanville Group.

This study uses a multi-proxy approach in an attempt to resolve an important lacuna in our knowledge of biological and geochemical events at the most critical time of early animal evolution. In so doing, this will test the validity of the global Cambrian chemostratigraphic curve at a point that coincides with the largest positive carbon-isotope shift recorded in the lower Cambrian period.

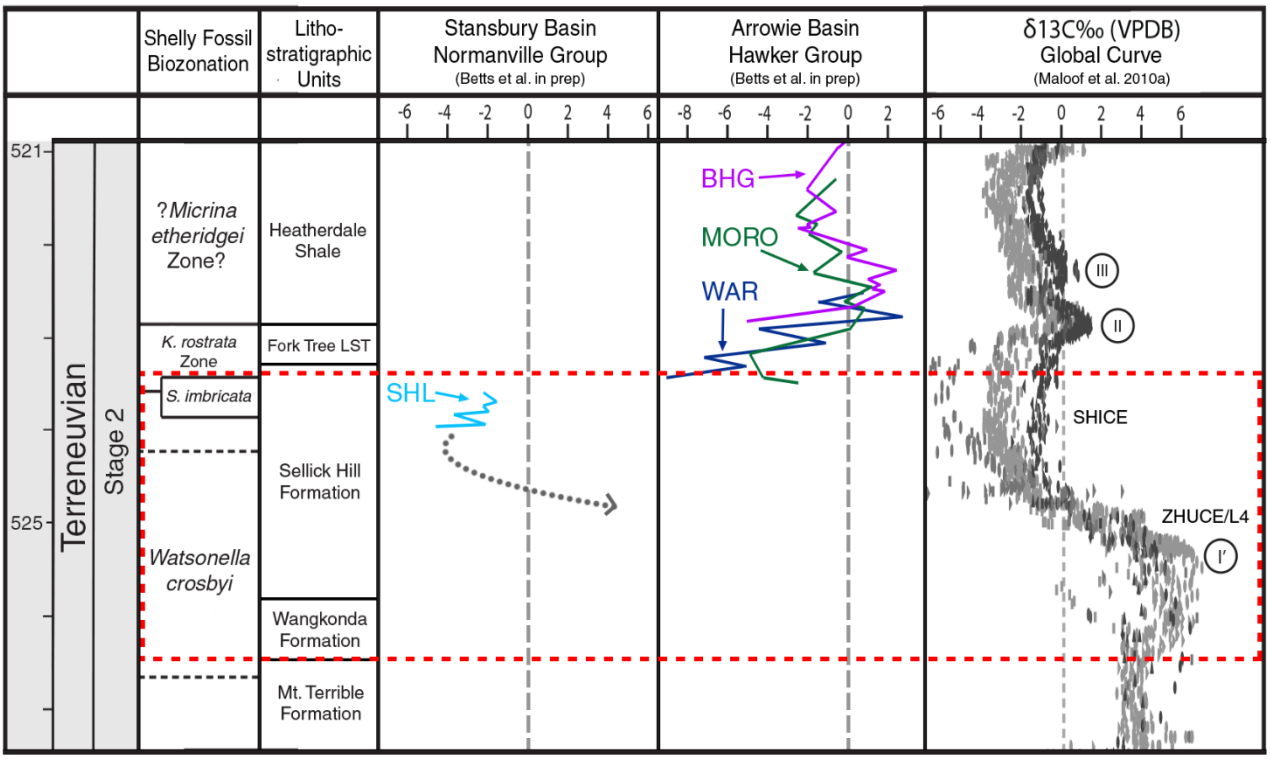

Figure 4. Lower Cambrian (Terreneuvian, Stage 2) shelly fossil biozonation of Jacquet *et al.* (in press) for the Eastern Stansbury Basin (Normanville Group) and Betts *et al.* (2016) for the Arrowie Basin (Hawker Group). Lithostratigraphic units of the Normanville Group indicated. Chemostratigraphic data from the Stansbury Basin (SHL section) and Arrowie Basin (MORO, BHG, WAR) from Betts *et al.* (in prep.) compared to the global chemostratigraphic curve of Maloof *et al.* (2010*a*) with carbon isotopic peaks indicated. Dotted arrow below SHL section is the predicted positive carbon isotopic excursion of Betts *et al.* (in prep.) which is the focus of this study (red boxed area). Modified from Jacquet *et al.* (in press).

1.e. Locality

This study was located in south-east South Australia, on the Fleurieu Peninsula within the eastern Stansbury Basin. Sampling focussed specifically on the lowermost carbonates of the Normanville Group: a lower Cambrian carbonate package that outcrops along a 16 km stretch of coastline, around 50 km south of Adelaide, bearing NE-SW (Fig. 5). The section, named 'WANG' after the Wangkonda Formation was measured and sampled along a north-west oriented road cut through the geology by Southern Quarries, Sellicks Hill, off Main South Road as part of commercial quarrying activities.

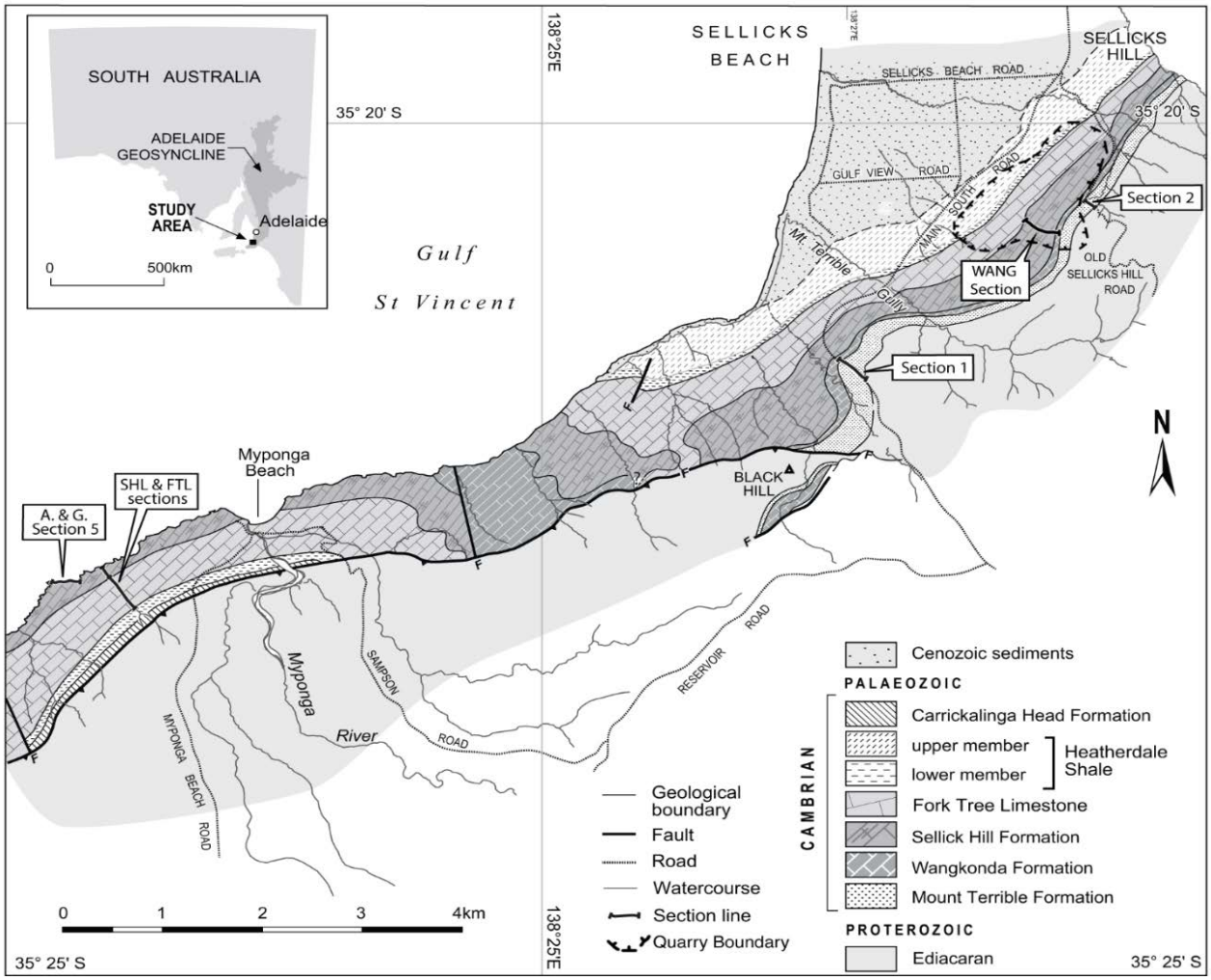

Figure 5. Regional geological map of the Normanville Group, South Australia. WANG section at top right, with previous sections indicated. Modified from Jacquet *et al.* (in press).

2. Geology and stratigraphy

The lower Cambrian age of South Australian carbonates has been known since the late 1800s (Tepper 1879; Etheridge 1890) and fossil identification began soon afterwards, beginning with archaeocyathids from the Flinders Ranges in the Arrowie Basin (Etheridge 1890) and the Fleurieu Peninsula in the eastern Stansbury Basin (Howchin 1897). The work of Howchin (1897) had provided the only means of dating the areas within the Stansbury Basin, largely until the significant discovery by Sprigg (1952) of Early Cambrian fossils of the Emu Bay Lagerstätte on Kangaroo Island; an area of outstanding preservation (Daily 1963). Howchin (1897) further noted that the successions of the area were extensively faulted, and sometimes reversed, a claim supported by Madigan (1925, 1927) after publishing a sketch map of the geology of the Fleurieu Peninsula and identifying overturn of these successions. Indeed, much of the section used in this project had a dip of 90°, and some minor overturn.

A preliminary lower Cambrian biostratigraphy for South Australia was first outlined by Daily (1956) who introduced 12 informal 'faunal assemblages' for regional correlation, mainly based on faunas from the Arrowie Basin. These assemblages became the baseline for studies of biostratigraphy and correlation in South Australia. The faunal assemblages were essentially 'informal', not having boundaries formally defined and most of the taxa were not treated taxonomically at the time so that stratigraphic ranges were poorly constrained. Abele & McGowran (1959) re-mapped the geology and defined the lithostratigraphy of the Cambrian succession on the Fleurieu Peninsula, identifying and naming four of the five lithostratigraphic units within the Normanville Group (in ascending order, the Wangkonda Formation, Sellick Hill Formation, Fork Tree Limestone and Heatherdale Shale.

Abele & McGowran (1959) identified the lowest member of their Wangkonda Formation as 'lower *Hyolithes* sandstone'. This ~92m thick package of dominantly bioturbated sandstones underlying the calcareous rocks of the Wangkonda Formation were named and defined as the Mount Terrible Formation by Daily (1963). These five formations were collectively named the Normanville Group by Daily & Milnes (1973), as they stretch between the Sellicks Hill and Normanville regions of South Australia (Fig. 5) These studies provided detailed depositional and sedimentological context of the area, identifying a gradual change in grain-size from coarse to fine from the Wangkonda Formation up through the Fork Tree Limestone and Heatherdale Shale. This change in grain-size corresponds to marine transgression throughout the Normanville Group (Alexander & Gravestock 1990, Gravestock *et al.* 2001). This study focuses on the lower Normanville Group, with special emphasis on collecting potential shelly fossils and

chemostratigraphic data from the carbonates from a section beginning just above the largely siliciclastic Mount Terrible Formation, passing completely through the Wangkonda Formation and overlying Sellick Hill Formation to just below the lower boundary with the Fork Tree Limestone. As such, only the Wangkonda and Sellick Hill formations will be described herein.

2.a. Wangkonda Formation

With the 'lower *Hyolithes* sandstone' of Abele & McGowran (1959) reassigned to the Mount Terrible Formation, the Wangkonda Formation is a 100-110 m thick unit of primarily blue-grey limestone containing laminate microbialites and dolostones, with coarse, clastic interbeds leached of carbonate (Abele & McGowran 1959) and quartz-rich clay near the base. Beds of oolitic and fenestral limestone indicate emergent (sub-aerial) exposure and therefore an extreme shallow water setting, which is not conducive to faunal diversity and also lowers fossil preservation potential (Gravestock & Gatehouse 1995; Gravestock *et al.* 2001). Indeed, limited fossil material has been recovered from the Wangkonda Formation. A few chancelloriid sclerites were reported in previous studies (Gravestock *et al.* 2001) as well as some sclerite fragments of *Australohalkieria* sp. (=*Halkieria* sp. of Figure 49 in Bengtson *et al.* 1990). Abele & McGowran (1959) indicated no biological activity was noticeable within the Wangkonda, but the studies of Gravestock *et al.* (2001) indicated the unit was highly bioturbated, though an extensive analysis of the sedimentology was not provided. The interbedding of the limestone and bioturbated, arkosic sandstone implies a peritidal sandflat setting. The boundary between the Wangkonda Formation and the overlying Sellick Hill Formation is commonly identified as 'sharp' (Daily 1969, Gravestock *et al.* 2001, Jenkins *et al.* 2002) but conformable.

2.b. Sellick Hill Formation

The Sellick Hill Formation has been documented in various localities, each with differing thicknesses due to excessive tectonism – the initial mapping of Abele & McGowran (1959) record its thickness as 180 m at Sellick Hill, 100 m at Carrackalinga Creek and 150 m at Myponga Beach, where Alexander & Gravestock (1990) record between 210 m and 260 m in their study. This study records the thickness at approximately 300 m. The Sellick Hill Formation was separated into five Facies Associations (A-E) by Alexander & Gravestock (1990). Facies Associations A and B are both around 40 m in thickness. Facies Association A consists of coarse arkosic sandstones and siltstones with minor bioturbation, whereas Facies Association B has finer, more calcareous

sandstone interbedded with siltstone and shales, and exhibits extensive bioturbation. Facies Associations A and B correspond to an inner shelf depositional system (Mount & Kidder 1993). Facies Associations C-E resemble a low-energy, carbonate ramp environment (Fig. 6). Facies Association C (90 m) contains ribbon limestones and calcareous shales, phosphatic hardgrounds and potential omission surfaces with quartz silt interbeds. Facies Association D is a very thin (~3 m) unit of mainly reefal archaeocyathid and fossil debris, potentially reworked reflecting rapid erosion from a high energy event or events. The topmost Facies Association E is ~80 m in thickness and is very similar to Facies Association C in deposition, except with less evidence of hardground surfaces with the addition of small archaeocyathid bioherms surrounded by ribbon and nodular limestones resulting in prominent, layered outcrops (Fig. 7).

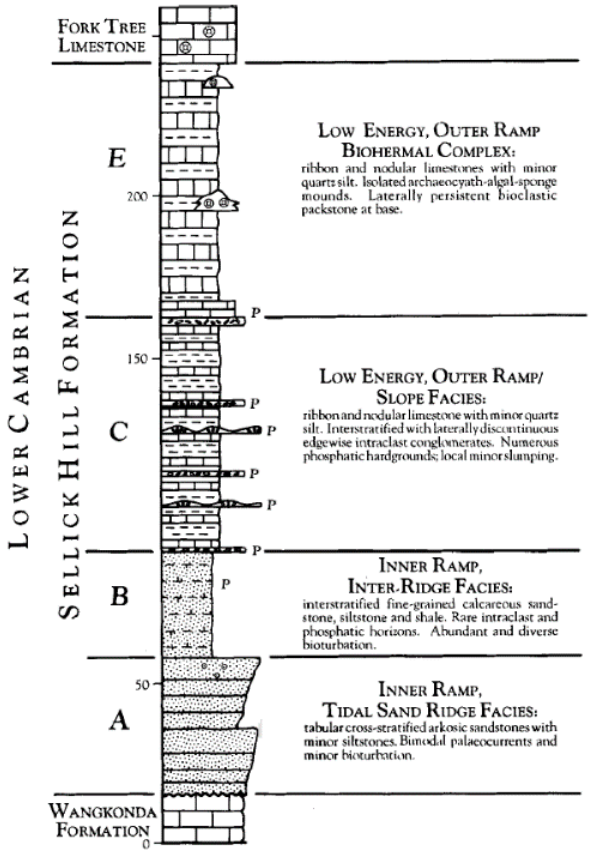

Figure 6. Facies Associations A-E of the Sellick Hill Formation. Sourced from Mount & Kidder (1993).

Figure 7. A prominent typical outcrop of Facies Association E carbonate of the Sellick Hill Formation. C. P. Mathewson (2016).

2.c. Previous biostratigraphic work

The sedimentological and depositional environment work of Alexander & Gravestock (1990) included basic fossil occurrence data, but the first real taxonomy of fossils from the Stansbury Basin was provided by Bengtson *et al.* (1990) who compiled a compendium of key shelly fossils from South Australia. This work was primarily based in the Arrowie Basin, but some data from the Normanville Group was included. Archaeocyathid faunas of the Sellick Hill Formation and Fork Tree Limestone described by Debrenne & Gravestock (1990) provided broad relative dating and some correlation with the Arrowie Basin. However, the first major biostratigraphic study of the Stansbury Basin was that of Gravestock *et al.* (2001), who expanded upon previous works and refined much of the taxonomy and sedimentology of the area, providing the baseline for all subsequent studies.

The thick marine carbonate deposits of South Australia, both in the Arrowie and Stansbury Basins, provide excellent insight into the organophosphatic and secondarily phosphatised facies of pre-trilobitic Terreneuvian Series and Cambrian Stage 2, comprising mainly SSFs. They are the only localities in Australia with evidence of this age and as such are incredibly significant. With the chronostratigraphic potential of SSFs still uncertain, there has been a concerted effort in refining their taxonomy and biostratigraphy within South Australia (Skovsted *et al.* 2007, 2008, 2009, 2011*a*, *b*, 2012, 2014, 2015; Jago *et al.* 2012; Topper *et al.* 2013; Larsson *et al.* 2014; Betts *et al.* 2015). Most of this work was performed within the Arrowie Basin, although the Fleurieu Peninsula of the eastern Stansbury Basin was the site of a trace fossil study which confirmed the Early Cambrian age of the Kanmantoo Group overlying the Normanville Group (Jago & Gatehouse 2007). Only one biostratigraphic study has been performed within the Normanville Group of the Fleurieu Peninsula since the work of Gravestock *et al.* (2001).

Based on a measured section by T. Brougham (unpub. Honours thesis, Macquarie University, 2009) that resampled and extended upon Section 5 of Gravestock *et al*. (2001), Skovsted *et al*. (2015) have been able to re-examine the biostratigraphy of the upper Normanville Group (upper Sellick Hill Formation through the Fork Tree Limestone to the Heatherdale Shale) using revised taxonomy of key shelly fossil taxa, especially species of the regionally widespread tommotiid taxon, *Dailyatia*. However, this study was focussed on the upper Normanville Group (top of the Sellick Hill Formation through to the base of the Heatherdale Shale), so the age of the lower Normanville Group is reliant on outdated, incomplete or erroneous faunal data which hinders regional correlation. The results of this study will intend to add considerably to this knowledge gap and provide an up-to-date view of lower Normanville biostratigraphy.

3. Materials and methods

3.a. Sample collection

Samples were collected every 5-10 m along a 404 m (tape distance) stratigraphic section ('WANG' after Wangkonda Formation) measured along a newly cut access road in Southern Quarries off Main South Road, Sellicks Hill, South Australia on the 6th February, 2016 (Fig. 8). At each sample location, two types of sample were collected: one to be leached with acetic acid to retrieve and determine microfossil material, and one for lithological and geochemical analyses (polished blocks and isotopic compositions). Samples were collected from *in-situ* vertically dipping (85-90° to slightly overturned) rocks and transported to Macquarie University. GPS locations were recorded, using a GARMIN handheld GPS module (Montana 650t) every 50 m from the start of the section, to identify offsets, and at the end of the section (Fig. 8). Descriptions of the lithology were recorded at each sample point, highlighting any lithological changes.

Figure 8. Aerial view of Southern Quarries with the WANG section and surrounding roads indicated. Arrow indicates direction up section.

3.b. Acid leaching

The technique used for optimal phosphatic fossil extraction follows the methods of Jeppsson *et al.* (1999) used in multiple acid leaching procedures to isolate Cambrian microfossils (e.g. Devaere *et al.* 2013; Sato *et al.* 2014; Skovsted *et al.* 2008, 2015). All acetic acid work was performed in the MQU Acid Leaching Facility.

Figure 9. The 14 L rectangular tubs used, with shallower basket nested within and lid behind. C. P. Mathewson (2016).

Before acid processing, all samples had a small lithological section removed, each which were transferred to individual, labelled bags for later isotopic analysis. Remaining microfossil samples were first cleaned with tap water to remove any excess soil, lichen and particulate residue, and placed in individual plastic mesh baskets which nested within 14 L rectangular plastic tubs, one per sample (Fig. 9). Each tub was filled with a buffered 10% acetic acid solution (CH_3COOH; diluted to 1-part acetic acid, 9-parts water) and left under a fume extraction hood to dissolve the carbonate rock matrix. The dilute acetic acid was changed every 3-4 days to normalise pH for effective residue yield. All samples were washed in acetic acid twice (if not fully dissolving before that) then washed with water, dried and put back into their bags for archiving.

All insoluble residues were wet sieved into coarse (>250 µm) and fine (>63 µm) fractions and decanted into aluminium trays where the samples were soaked in de-ionised water to remove all traces of acid. The samples were oven dried at 50°C overnight and transferred to labelled specimen jars. Samples were picked using a fine-tipped paintbrush under a stereo dissecting microscope (Olympus SZ40) and all microfossil specimens were stored in labelled three-well micropalaeontological slides with glass covers (Fig. 10).

Figure 10. Olympus SZ40 stereo dissecting microscope with three-well slide.
C. P. Mathewson (2016).

After picking through all the samples once, those which yielded identifiable fossil material (>20% of sample yielded fossils) were put through the washing process again until all material was completely dissolved. After all samples had been picked, the slides were closely examined to identify the fossils to species-level if possible. Well-preserved microfossils were mounted on labelled pin-type stubs with conductive carbon adhesive tabs for imaging on a scanning electron microscope. The microfossil material retrieved from the first two washes was quite fragmentary (although had a good yield). The methodology changed slightly for the second set of washing to extinction, by using solely the coarse (>250 μm) sieve to try to limit the amount of fragmentation occurring in the sieving process of the washing itself. It was marginally faster to go through the samples but had no change in fragmentation.

3.c. Imaging techniques

Selected specimens were mounted on pin-type stubs, sputter coated with a fine (<1 μm thick) layer of gold using an EMITECH K550 sputter coater and scanned at the MQU Microscopy Facility under a variable pressure JEOL JSM-6480 scanning-electron microscope (SEM) for fine-scale, high-resolution images. Specimens were tilted, zoomed and rotated for clarity of particular areas of interest.

3.d. Polished blocks

All lithological samples from each sample location were cut with a diamond saw. Each block was cut to a maximum size of 40 x 20 x 10 mm (L x W x D) and labelled with its original ‘way- up’ orientation (youngest at top of sample; Fig. 11). Small, cleanly cut parts of each sample were put aside in individual, labelled bags for isotopic analysis, along with the few from the microfossil samples, for a total of 48 isotopic samples. Blocks revealing key features of the Wangkonda and Sellick Hill Formations, including the different Facies Associations (A-E) of Alexander & Gravestock (1990) were polished using 800-grit sandpaper in the Macquarie University Palaeobiology Lab.

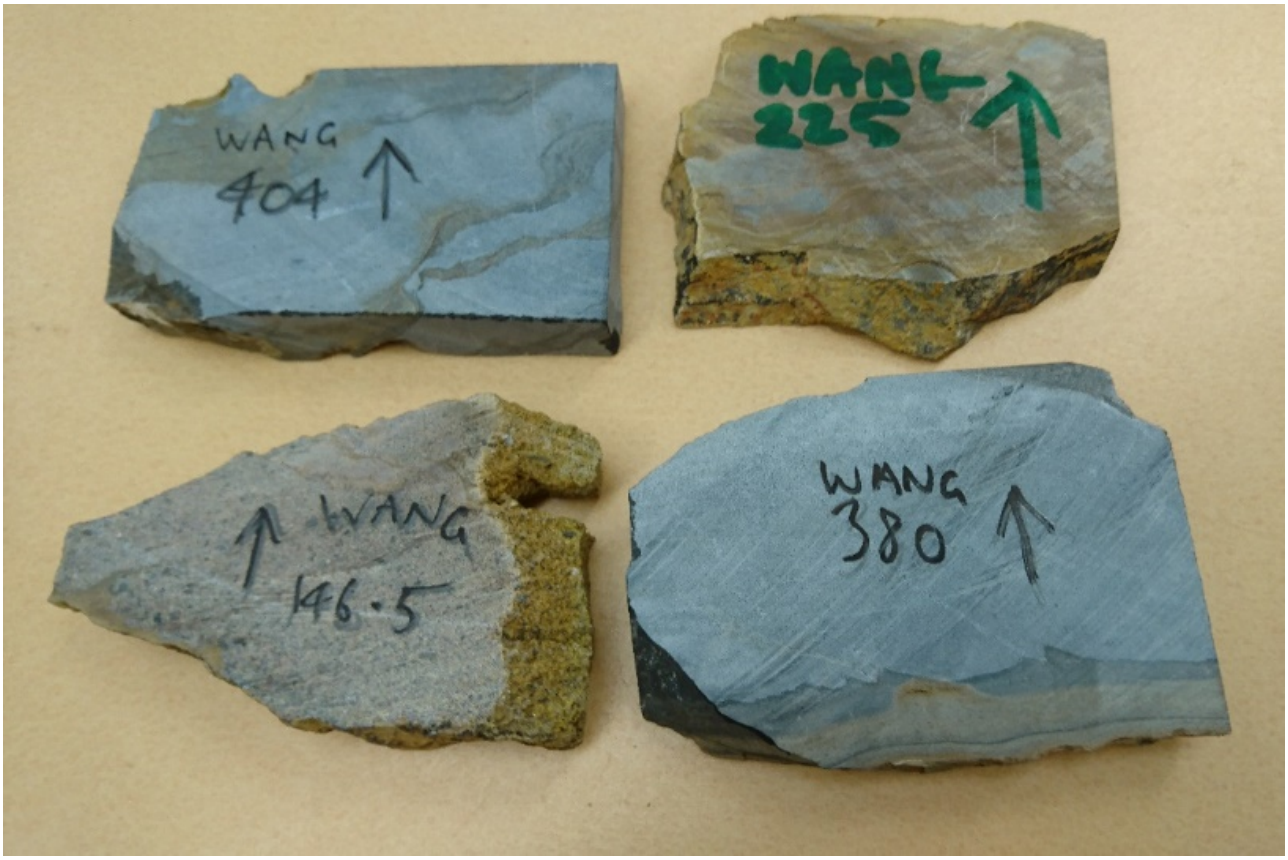

Figure 11. Examples of cut blocks with ‘way-up’ orientation arrow. C. P. Mathewson (2016).

3.e. Isotopic analysis

Freshly cut faces of the lithological samples were cleaned with ethanol (C_2H_5OH, 96%) to remove any dust and other contaminants. A homogeneous region of fine grained (micritic) carbonate was selected for each sample using a microscope, and 15-20 mg of carbonate powder was drilled out using a low speed Dremel Digital 400-series with fine drill-heads of various shapes (Fig. 12, inset), depending on the hardness of the sample. Paper placemats were used to catch the powders and discarded after every sample to remove any chance of cross-sample contamination. The powders were transferred to individual, labelled, tapered, plastic vials (Fig. 12). After each sample was drilled, the drill bit was cleaned with ethanol to remove any residual powder.

The powders in vials were taken to the University of Adelaide in South Australia for mass spectrometry. A total of 100 powders were used in the process: 48 samples plus 24 random replicates, 27 standards and one blank. The standards ensured mass spectrometry calibration for size (small and large) and drift (time). Size was calibrated with the weight of each sample lying somewhere in between the small and large weights of the standards (~50-150 µg). Drift was calibrated by grouping standards at the start and end of the set (and variously throughout) so the

Figure 12. Dremel, a labelled vial and a sample with drilled-out powder. Inset: a selection of used drill bits. C. P. Mathewson (2016).

unknown sample values would lie between the known standard values. Each vial was purged to replace the air inside each vial with helium, which is inert. Ten drops of 103-105% phosphoric acid (H_3PO_4) was added to each vial to release carbon dioxide gas, which separated into its constituent ions as it passed through the mass spectrometer. After the process was completed, the data were corrected using the standards as a baseline – the standards should have equal values throughout the data set, so any variations in the standards from instrumental error can be accounted for. The corrected data points were aligned with a stratigraphic column over a zero-line, and a smooth curve was drawn between each point, for both the oxygen and carbon-isotope data (Fig. 23 in *Chemostratigraphic results*).

4. Results

4.a. Lithostratigraphic results

The 404 m long WANG stratigraphic section has its base (35° 20′ 38.9″ S, 138° 28′ 25.9″ E) at the boundary between the Mount Terrible and Wangkonda Formations (=WANG/0.0; Figs. 13, 15) passing through the Wangkonda Formation (98 m) and Sellick Hill Formation (306 m). The top of the section in the Sellick Hill Formation occurs 404 m above the base of the section, ~5-10 m below the lower boundary of the Fork Tree Limestone which has been removed by large scale quarrying activities. The strata dip at 90° (± 2°) throughout the entire WANG section (e.g. Fig. 14).

Figure 13. The base of the WANG section (WANG/0.0) at the Mount Terrible-Wangkonda Formation boundary. C. P. Mathewson (2016)

The five Facies Associations described by Alexander & Gravestock (1990) can be readily identified in the WANG section based on preliminary lithological comparison of polished blocks (Fig. 15). Facies Association A is characterised by red-brown, muddy siltstone in ripple-like patterns, which identify with the lithological samples between WANG/100.0 and 143.0, of a thickness very similar to the 41 m reported by Gravestock *et al.* (2001). Facies Association B occurs in two small samples, WANG/143.0 and 146.5, however it has a total thickness of 30-40 m. These samples exhibit a change to heterolithic, medium-grained sandstone and siltstone, with variously preserved examples of the trace fossil *Treptichnus* isp. previously reported in abundance within Facies Association B (Gravestock *et al.* 2001).

Figure 14. The sampled quarry wall ~200 m above the base of the WANG section, within Facies Association C of the Sellick Hill Formation, showing a dip of ~90°. C. P. Mathewson (2016).

Facies Association C within the WANG section has its base at approximately WANG/167.0, ranging to approximately WANG/321.0; a total thickness of 154 m. This thickness is markedly different from that reported in previous studies (e.g. 90 m in Gravestock *et al.* 2001), however within the WANG section, Facies Association C contains a 13 m thick (WANG/283.0-296.0) translocation and potential repetition. The polished blocks reveal the much darker grey ribbon limestone (Fig. 15). The lower half within WANG contained one partial, conical hyolithelminthid tube (WANG/190.0; Fig. 22a). Facies Association D occurs within a relatively narrow 10 m interval between WANG/321.0 and 331.0, characterised by dark grey, nodular limestone with undulating, calcareous mudrock layers. WANG/321 aligns with the first recovered appearances within the section of a comparatively diverse range of taxa. The lower boundary of Facies Association E occurs at WANG/331.0, located some 73 m from the top of the section (WANG/404.0), and is identified by its characteristic nodular ribbon limestone throughout the whole thickness. Though not the core focus of this study, preliminary lithostratigraphic analysis does reveal the basic depositional environment of the section, and confirms that the previous sedimentological interpretations and lithofacies associations identified by Alexander & Gravestock (1990) and Mount & Kidder (1993) can be identified in the WANG section.

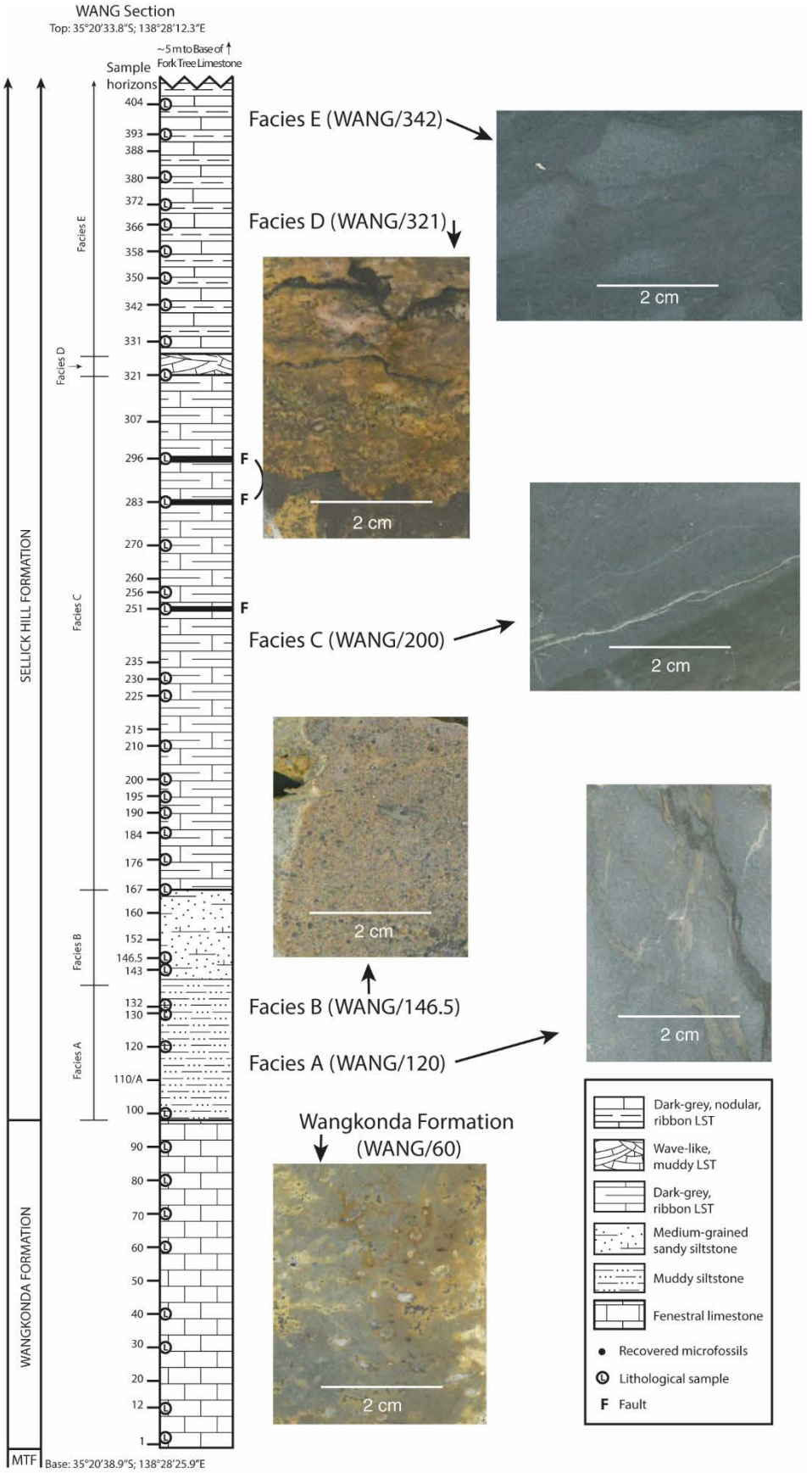

Figure 15. The lithostratigraphy of the WANG section, with section line and Facies Associations on the left, and lithological polished blocks at right. All polished blocks have their orientation upwards. Photos by C. P. Mathewson (2016).

4.b. Biostratigraphic results

The biostratigraphy of the WANG section is presented in Figure 16. Fossils are very scarce in the very shallow water (supratidal) Wangkonda Formation. Bengtson *et al.* (1990, Fig. 49) figured some poorly preserved, indeterminate halkieriid sclerites (?*Australohalkieria* sp.) from the Wangkonda Formation and Gravestock *et al.* (2001, p. 48) reported *Chancelloria* sclerites from near the top of the unit at Myponga Beach. Low yields of microfossils in the Wangkonda Formation as represented in the WANG section is thus not unexpected and conforms to previous reports, with only a single tube cf. *Torellella* sp. recovered from 60 m above the base of the section (WANG/60.0). This genus has a long range from Cambrian Stage 2 through to Stage 4 within Australia (Gravestock *et al.* 2001) and elsewhere and so has no real biostratigraphic signal. Unfortunately no other shelly fossil material was recovered from within the 98 m of Wangkonda Formation. However, past studies by Daily (1976) and Gravestock *et al.* (2001, p. 48) and a recent report from Jacquet *et al.* (in press) also noted the presence of vertical trace fossils belonging to *Skolithos* sp. and/or *Diplocraterion* sp. 'piperock' in more sandy layers within the unit, suggesting correlation with similar 'piperock' in the Parachilna Formation in the Arrowie Basin and aligning these units with the incoming of vertical burrowing characteristic of Cambrian Stage 2 (Mángano & Buatois 2012).

The contact between the Wangkonda Formation and the overlying Sellick Hill Formation is sharp and appears conformable in the WANG section. Gravestock *et al.* (2001, p. 48) also report a sharp, conformable contact at this level at Myponga beach. Much like the underlying Wangkonda Formation, Facies Association A of the lower Sellick Hill Formation is also very poorly fossiliferous in the WANG section. Gravestock *et al.* (2001) reported the presence of the molluscs *W. crosbyi* and *Mackinnonia rostrata* (Zhou & Xiao 1984) along with hyolithelminthids, chancelloriids and halkieriids in lowermost Facies Association A and an even more diverse molluscan fauna including *Figurina nana* (Zhou & Xiao 1984), *Anuliconus truncatus* (Parkhaev 2001), *Obtusoconus brevis* (Esakova & Zhegallo 1996) and *Stenotheca drepanoida* (He & Pei 1984) in the upper part of Facies Association A. Unfortunately, apart from the presence of indeterminate hyolithelminthids, none of the molluscs reported by Gravestock *et al.* (2001) were recovered from Facies Association A in the WANG section. Some of the taxa reported from the upper part of Facies Association A of the Sellick Hill Formation by Gravestock *et al.* (2001) such as *Halkieria* (=*Australohalkieria*) *parva* (Conway Morris), *Thambetolepis* (=*Sinosachites*) sp., *Cupitheca* sp. and chancelloriids do occur in Facies Associations D and E of the Sellick Hill Formation in the WANG section, but are not present in lower levels.

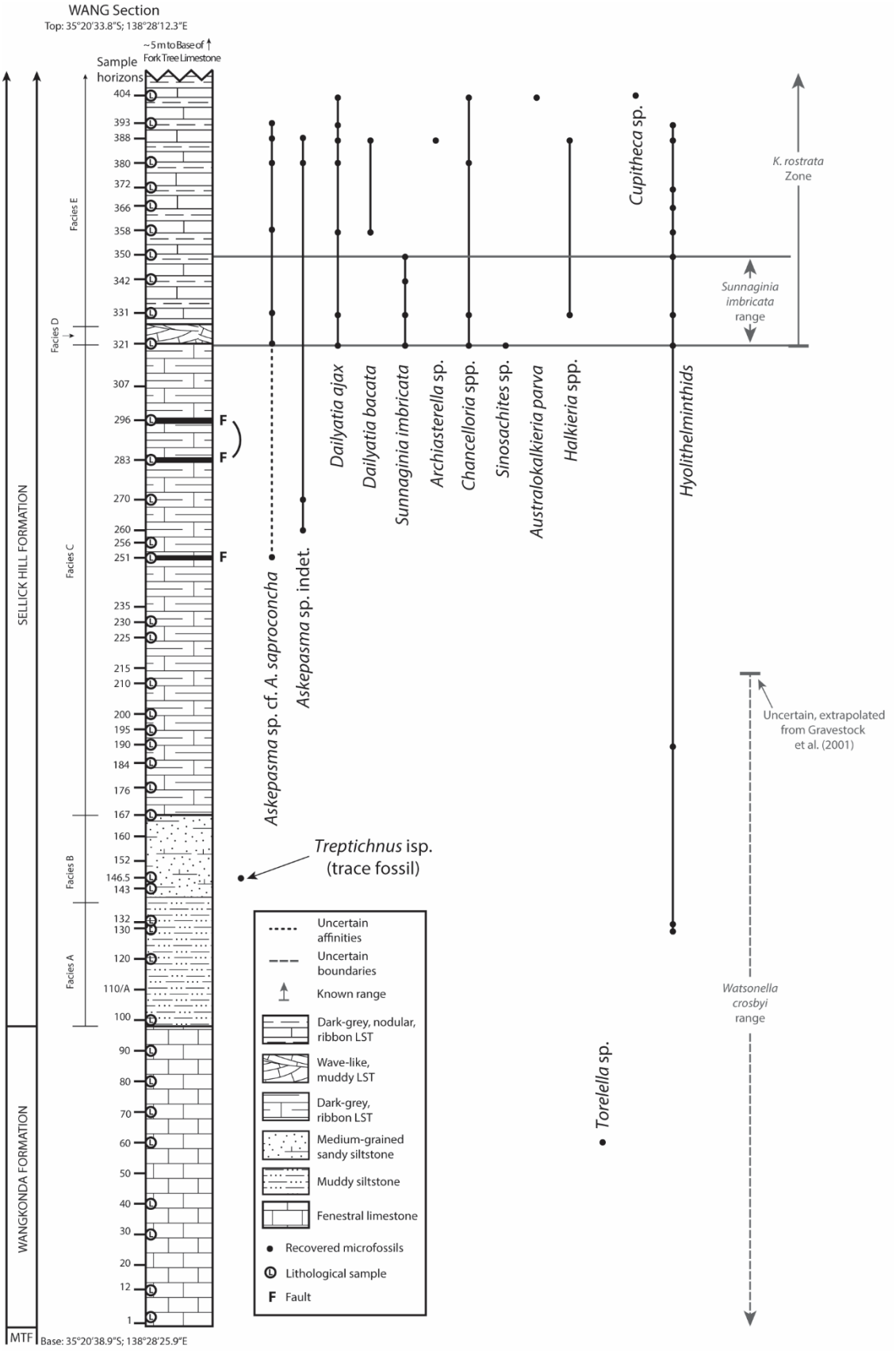

Figure 16. WANG stratigraphic section through the Wangkonda and Sellick Hill Formations in the eastern Stansbury Basin. Ranges of shelly taxa indicated. Interpreted Facies Associations A-E of Alexander and Gravestock (1990) are indicated left of lithostratigraphic column. The *K. rostrata* Zone and ranges of *S. imbricata* and *W. crosbyi* are indicated.

Trace fossils present in the cross-bedded sandy beds of Facies Association B are dominated by horizontal traces including *Treptichnus* isp. (Fig. 17). Gravestock *et al.* (2001) additionally report (but do not figure) *Monocraterion*, *Plagiogmus* and *Taphrelminthopsis* from Facies Association B in their Section 5 at Myponga Beach.

Figure 17. Horizontal trace fossil *Treptichnus* isp. from WANG/146.5, typical of Facies Association B. Centimetre ruler as scale bar. C. P. Mathewson (2016).

Paterinid brachiopod fragments were recovered from WANG/321.0 (Facies Association D) through to the top of the section (Facies Association E) within the Sellick Hill Formation, and were identified as *Askepasma* sp. cf. *A. saproconcha*. Notably, specimens predominantly represented juvenile growth stages, where the diagnostic median fold in the dorsal valve and sulcus in the ventral valve has not yet developed (see Fig. 4F in Topper *et al.* 2013). There was one small fragment within WANG/251.0 cautiously attributed to the same species (Fig. 18a, as compared to 18b; Topper *et al.* 2013), however it was a very thin-shelled, fragmentary specimen so this classification is still uncertain. A number of relatively poorly preserved, very thin-shelled paterinid brachiopod fragments attributed here to *Askepasma* sp. indet. (Fig. 18h-n) were recovered from a 10 m thick succession in the upper half of Facies Association C (WANG/260.0 to WANG/270.0) and at WANG/380.0 within Facies Association E. Those from Facies Association E have well developed, thickened, concentric lamellae (Fig. 18h, i) that are quite different to *Askepasma* sp. cf. *A. saproconcha*, and the fragmentary nature of the shells makes identification difficult. The

characteristic micro-reticulate ornament is also not apparent in *Askepasma* sp. indet. or *Askepasma* sp. cf. *A. saproconcha*, though this could be attributed to the relatively poor state of preservation and so a more cautious approach in the identification of *Askepasma* sp. cf. *A. saproconcha* is taken.

The camenellan tommotiid taxa *Dailyatia ajax* (Fig. 19a-s) and *D. bacata* (Fig. 19t-x) were recovered from WANG/321.0 up to the top of the section. The presence of *S. imbricata* (Fig. 20), previously linked with Facies Association D (Gravestock *et al.* 2001) is confirmed and the range of this taxon occurs in Facies Associations D and E, over 29 m from WANG/321.0 to WANG/350.0 in the section (Fig. 16). Other taxa occurring within Facies Associations D and E of the section include chancelloriids (Fig. 21a-f), *Archiasterella* sp. (WANG/388, Fig. 21g), the hyolithid *Cupitheca* sp. (WANG/404.0, Fig. 22h) and palmate, cultrate and siculate sclerites of halkieriids including *Australohalkieria parva* (Fig. 22i-m).

Figure 18 (below). *Askepasma* species from the WANG section, Sellick Hill Formation

(a) plan view, *Askepasma* sp. cf. *A. saproconcha*, WANG/251.0, MPAL00538 (b) *A. saproconcha*, SAMP47084, Chace Range CR1-136, from Topper *et al.* (2013) Fig. 4A, white dotted line compares to A (this study) (c-f) plan views of *Askepasma* sp. cf. *A. saproconcha* larval shells. (c) WANG/251.0, MPAL00539. (d) WANG/358.0, MPAL00540. (e) WANG/321.0, MPAL00541. (f, g) WANG/380, MPAL00542 (g) 270x zoom of external ornament. (h-n) *Askepasma* sp. indet. (h, i) plan view, WANG/380.0, MPAL00543 (i) 250x zoom of external ornament. (j, k) internal view (basal/ventral view?), WANG/388.0, MPAL00544 (k) 300x zoom of internal ornament. (l, m) plan view, WANG/388.0, MPAL00545 (m) 160x zoom of external ornament. (n) plan view, WANG/388.0, MPAL00546.

Figure 19 (below). *Dailyatia* sclerites from the WANG section, Sellick Hill Formation

(a-s) *D. ajax* sclerites (a) A-sclerite, plan view, WANG/321.0, MPAL00547. (b) lateral view, WANG/321.0, MPAL00548. (c) internal, WANG/321.0, MPAL00549. (d) lateral view, WANG/321.0, MPAL00550. (e, f) A2-sclerite?, oblique view, WANG/321.0, MPAL00551 (e) zoomed in on external ornament. (g) lateral view, WANG/321.0, MPAL00552 (h, i) sinistral B1-sclerite?, anterior-lateral field?, WANG/380.0, MPAL00553 (i) zoomed in on external ornament. (j, k) lateral view, C-sclerite?, WANG/380.0, MPAL00554 (j) zoomed in on central plicae?. (l) lateral view, sinistral C-sclerite?, WANG/380.0, MPAL00555. (m, n) lateral view, C1-sclerites, WANG/388.0, MPAL00556, MPAL00557. (o, p) lateral view, WANG/388.0, MPAL00558 (o) zoomed in on recurved tip. (q, r) lateral view, subtriangular sclerite, WANG/404.0, MPAL00559 (q) zoomed in on tip. (s) oblique view, C-sclerite, WANG/404.0, MPAL00560. (t-x) *D. bacata* sclerites (t) lateral view, C-sclerite, WANG/388.0, MPAL00561. (u) plan view?, WANG/358.0, MPAL00562. (v) lateral view, C1-sclerite, WANG/358.0, MPAL00563. (w) plan view, fragmentary A-sclerite, WANG/358.0, MPAL00564. (x) lateral view, C1-sclerite, WANG/358.0, MPAL00565.

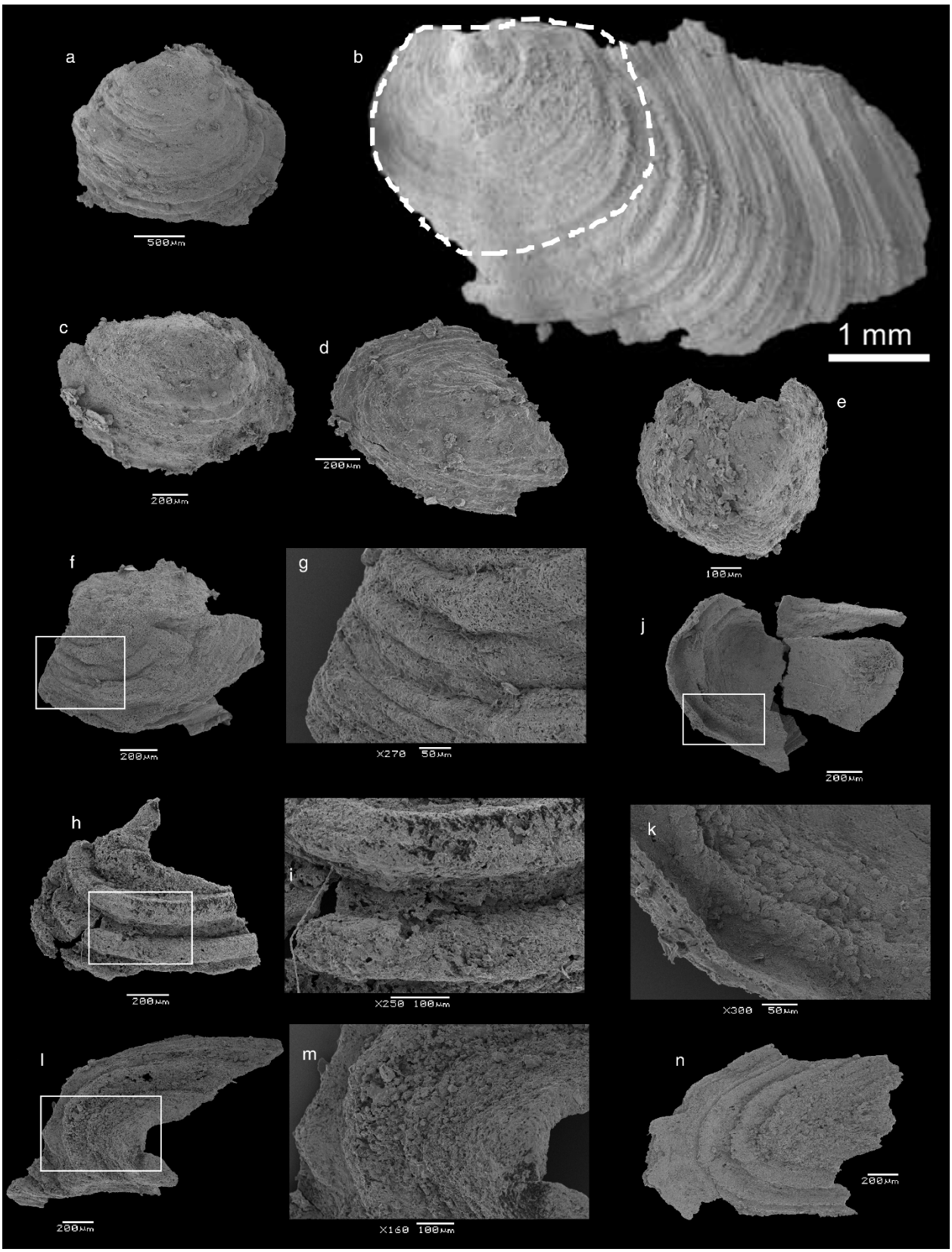

Figure 18. Caption above

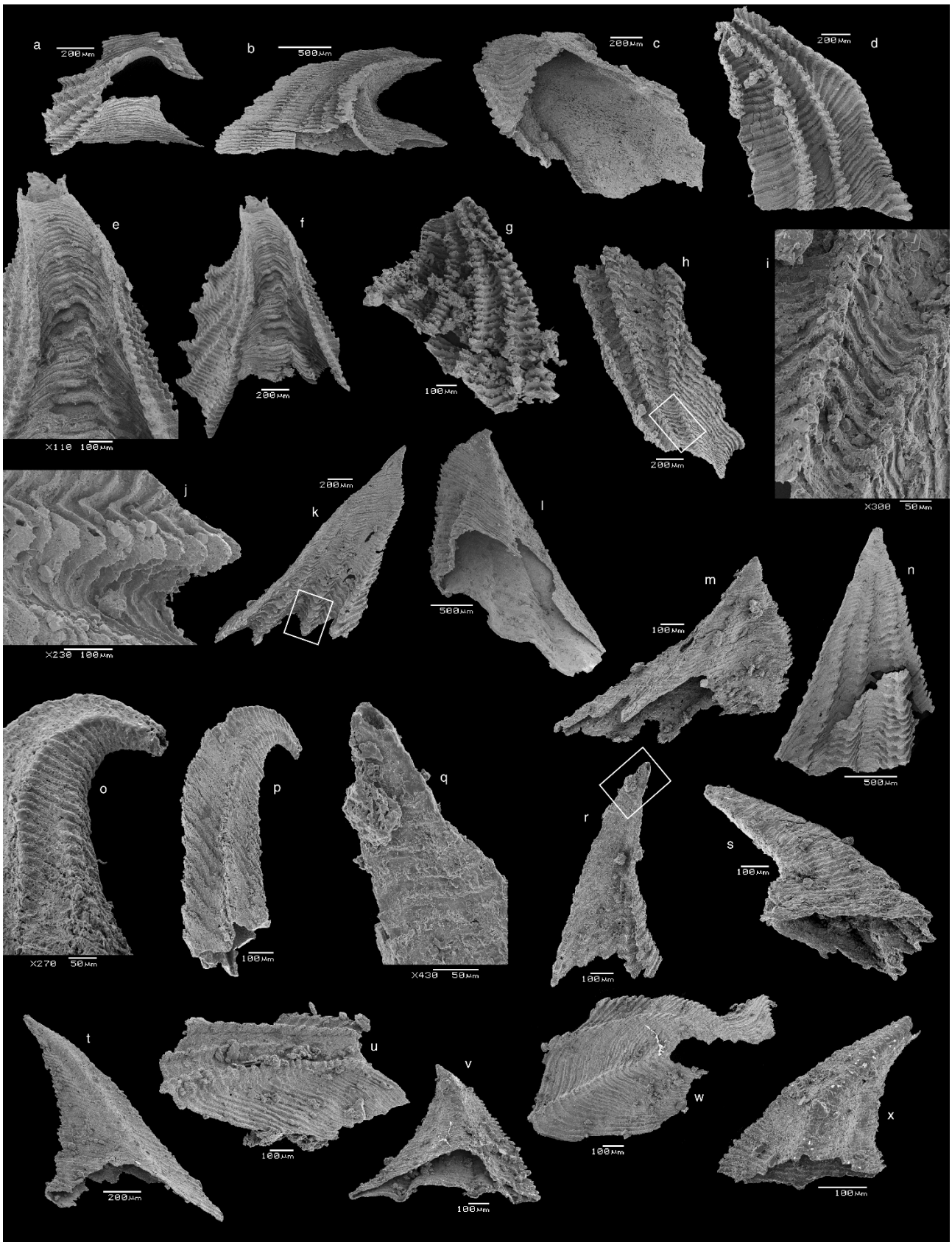

Figure 19. Caption above

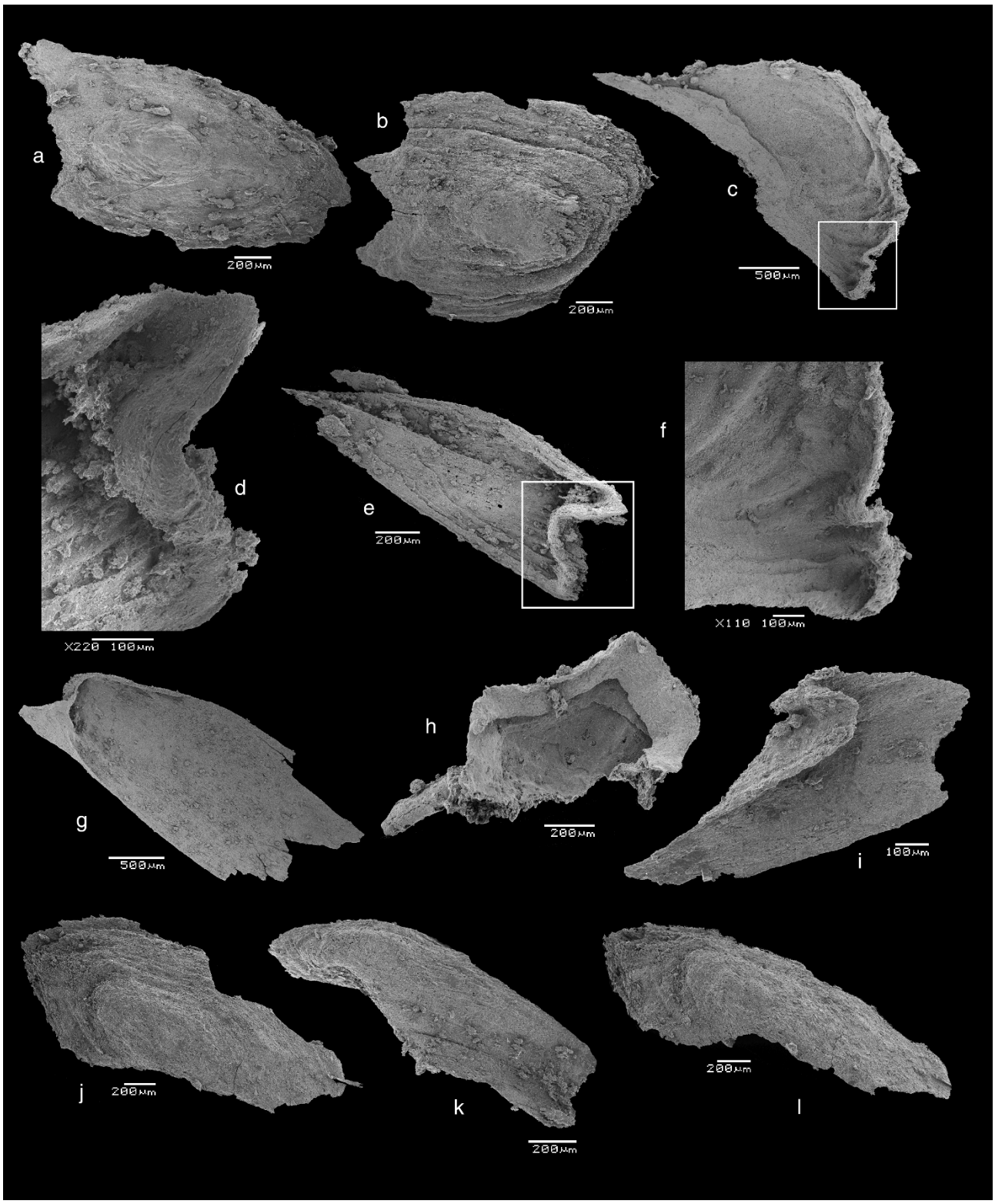

Figure 20. *Sunnaginia imbricata* from the WANG section, Sellick Hill Formation

(a-b) plan view, WANG/321.0, MPAL00566, MPAL00567. (c, f) basal view, WANG/321.0, MPAL00568 (f) zoomed on wrinkled interior texture. (d, e) basal view, WANG/321.0, MPAL00569 (d) zoomed on wrinkled interior texture. (g, h) basal view, WANG/321.0, MPAL00570, MPAL00571. (i) basal view, WANG/331.0, MPAL00572. (j-l) plan view, WANG/331.0, MPAL00573, MPAL00574, MPAL00575.

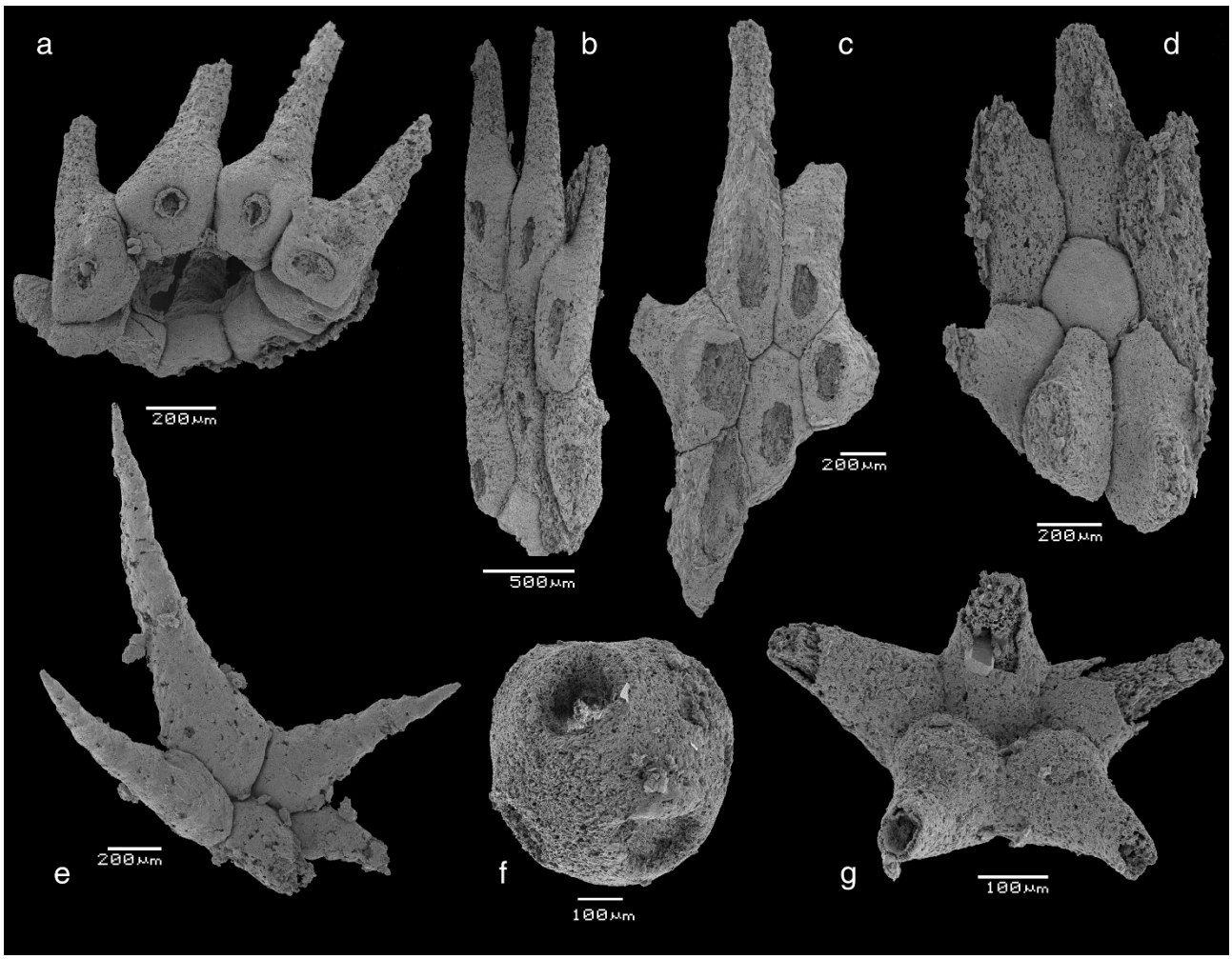

Figure 21. Chancelloriid fauna from the WANG section, Sellick Hill Formation

(a-f) Indeterminate chancelloriid sclerites. (a) oblique view, WANG/321.0, MPAL00576. (b) basal view, WANG/321.0, MPAL00577. (c) basal view, WANG/321.0, MPAL00578. (d) plan view, WANG/321.0, MPAL00579. (e) plan view, WANG/404.0, MPAL00580. (f) lateral view, WANG/388.0, MPAL00581. (g) *Archiasterella* sp., plan view, WANG/388.0, MPAL00582.

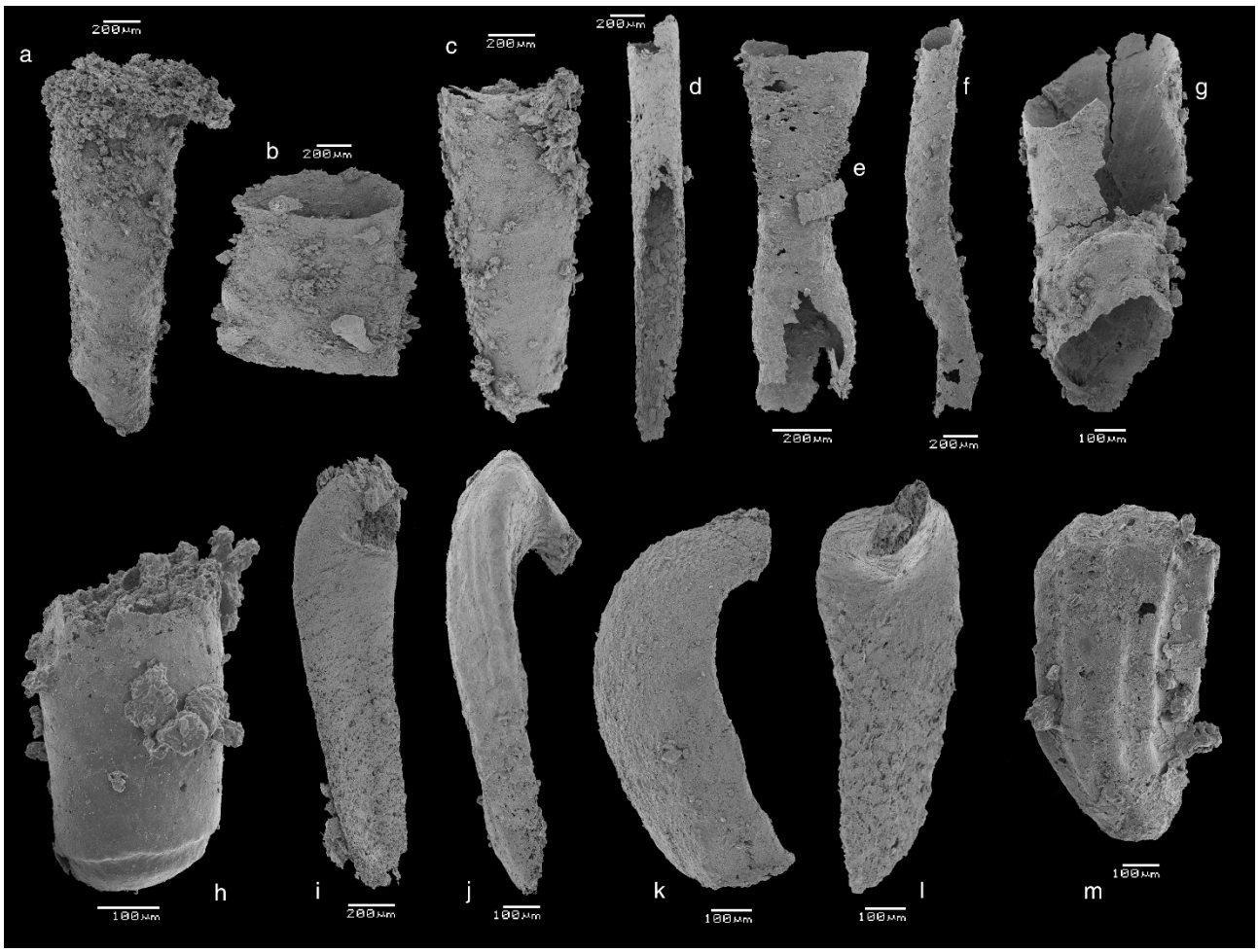

Figure 22. Halkieriid sclerites and hyolithelminthids from the WANG section, Sellick Hill Formation

(a-g) Indeterminate hyolithelminthids, lateral view; (a) WANG/190.0, MPAL00583. (b-d) WANG/321.0, MPAL00584, MPAL00585, MPAL00586. (e-g) WANG/358.0, MPAL00587, MPAL00588, MPAL00589. (h) *Cupitheca* sp., lateral view, WANG/404.0, MPAL00590. (i-l) Indeterminate halkieriid sclerites, lateral view, WANG/321.0. (i) cultrate sclerite, MPAL00591. (j) siculate sclerite, MPAL00592. (k) palmate sclerite, MPAL00593. (l) cultrate sclerite, MPAL00594. (m) *Australohalkieria parva*,, palmate sclerite, lateral view, WANG/404.0, MPAL00595.

4.c. Chemostratigraphic results

The chemostratigraphic curve for the WANG section is presented in Figure 23. Sample WANG/1.0 has an initial positive $\delta^{13}C$ value of 2.33‰, and the section has minor fluctuations about this value through the entire Wangkonda Formation, with a brief drop into negative values (WANG/80.0, -0.03‰; WANG/90.0, -1.20‰; standard errors and raw values in *Supplementary material*, Table S1, S2 below) before becoming positive (WANG/100.0, 2.00‰). This creates an initial positive peak of 4.56‰ at WANG/70.0. Within Facies Association A of the Sellick Hill Formation, the values become consistently more positive up section to WANG/120.0, where the $\delta^{13}C$ values reach the second, and highest, positive peak (5.70‰) in the section line. This peak also lies within the purported range of *W. crosbyi* (Fig. 23; see Jacquet *et al.* (in press) for details). The $\delta^{13}C$ values drop consistently throughout Facies Association B in the Sellick Hill Formation, passing into the negative where they plateau between WANG/152.0 and 167.0 (-1.22‰ and -1.37‰ respectively).

Three negative peaks occur within Facies Association C, over a stratigraphic thickness of 88 m, in a range between the first $\delta^{13}C$ value peak of -4.26‰ at WANG/195.0 and the third $\delta^{13}C$ value peak of -4.96‰ at WANG/283.0. The second, and most pronounced $\delta^{13}C$ value peak at WANG/215.0 and WANG/225.0 (-7.43‰ and -6.88‰, respectively) produced the lowest values, however these values are uncharacteristically low within a narrow range, so are treated with caution (see *5.a.2. Chemostratigraphy* below). After the third negative $\delta^{13}C$ value peak at WANG/283.0, the values gradually become more positive from the top of Facies Association C through to the end of the section where they reach 0.00‰ at the final sample of the section, WANG/404.0, within Facies Association E. The $\delta^{18}O$ curve closely follows a co-variant trend to the $\delta^{13}C$ curve, though some levels (WANG/146.5, 215.0, 225.0, 296.0 and 321.0), display opposing trends and peaks in $\delta^{18}O$ compared to the $\delta^{13}C$ curve.

Three sample horizons were excluded from both the carbon and oxygen curves. WANG/146.5 was not included in the curve as it was taken from a trace fossil sample off the main section line, and was heavily weathered and broken up by quarrying activities. The sharp negative $\delta^{13}C$ values and sharp positive $\delta^{18}O$ values of WANG/296.0 were excluded from the curve as they were taken from within a fault zone where there was significant dip change from deformational effects, thus potentially giving an uncharacteristic result. A negative $\delta^{13}C$ spike at WANG/321.0 was also excluded from the curve as it, and Facies Association D itself, was subject to significant erosion, possible reworking (see also Gravestock *et al.* 2001) and frequent sub-aerial exposure (or sediment starved omission surfaces) suggesting strong diagenetic change in these samples.

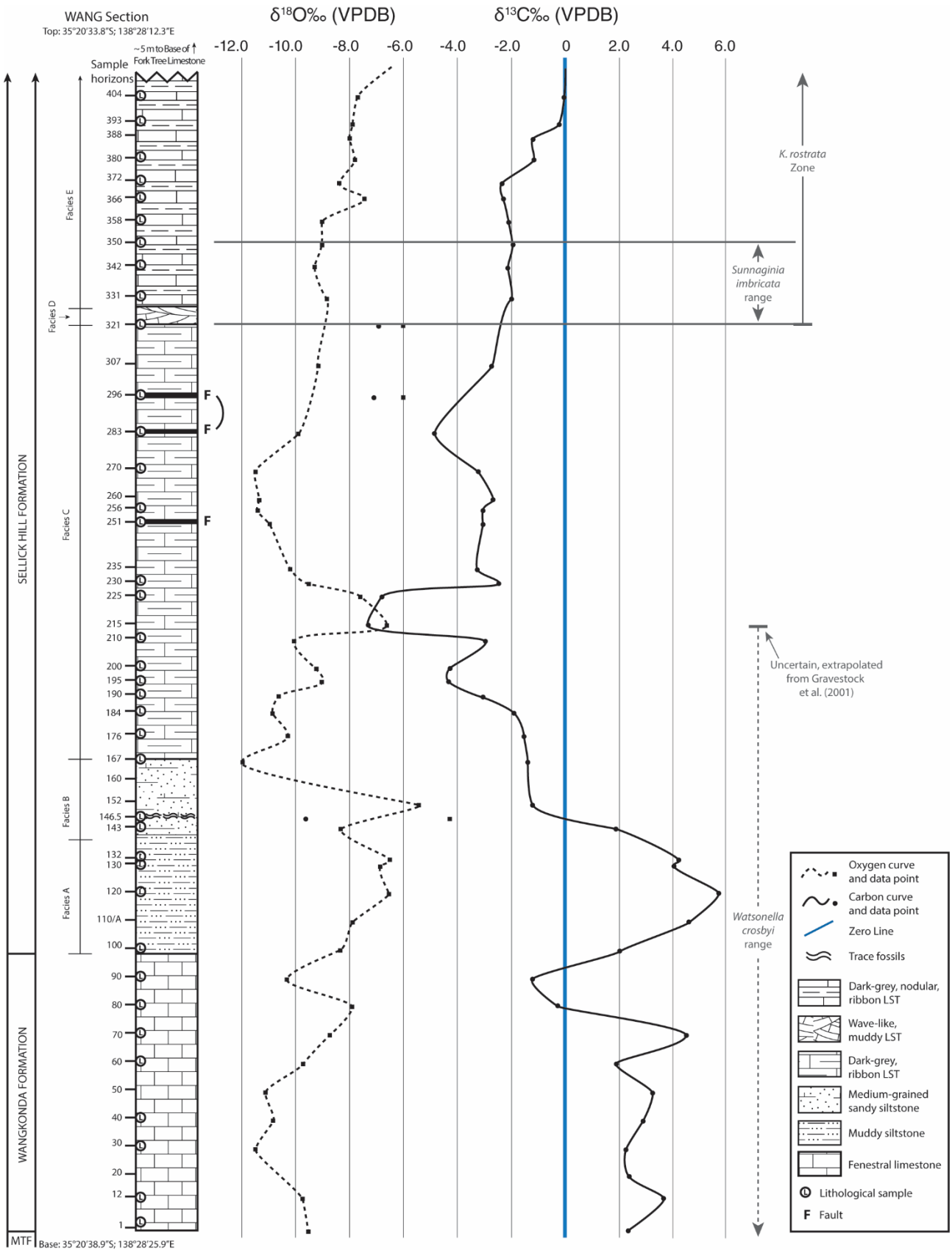

Figure 23. The $\delta^{18}O$ (left, dotted) and $\delta^{13}C$ (right, solid) isotope curves from the WANG section with stratigraphic column and Facies Associations (far left) and biozones (grey) included. Zero line in blue.

5. Discussion

The previous studies of Betts *et al.* (2016, in review, in prep.) successfully used a multi-proxy approach of chemo- and biostratigraphy to link endemic Australian faunas to the global chemostratigraphic curve and so constrained faunas of similar age around the globe, as well as demonstrated consistent reproducibility both within and between depositional basins (Maloof *et al.* 2010*a*). Betts *et al.* (2015, in prep.) also predicted that the ZHUCE $\delta^{13}C$ positive should potentially occur in the successions of the lower Normanville Group in the eastern Stansbury Basin which they considered to be older than the stratigraphic levels developed in the Arrowie Basin.

5.a. Interpretation of results

5.a.1. Biostratigraphy: Kulparina rostrata *Zone*

The *Kulparina rostrata* biozone, hereafter the *K. rostrata* Zone, was recently defined by Betts *et al.* (2016) as the oldest lower Cambrian shelly fossil zone in the Arrowie Basin succession in South Australia. The Zone is characterised by a relatively low-diversity shelly assemblage, typically containing five or six taxa including eccentrothecimorph and camenellan tommotiids and the paterinid brachiopod *Askepasma saproconcha* (Topper, Holmer, Skovsted, Brock, Balthasar, Larsson, Pettersson Stolk & Harper 2013). The lower boundary of the *K. rostrata* Zone is defined by either the first appearance of the eponymous *K. rostrata* or the paterinid brachiopod *A. saproconcha* (Betts *et al.* 2016, p. 172). Whilst *K. rostrata* was not recovered from the WANG section, this taxon was reported and illustrated from Facies Association E in the FTL section at Myponga by T. Brougham (unpub. Honours thesis, Macquarie University, 2009) and confirmed by resampling by Betts *et al.* (in press).

The prediction of Betts *et al.* (2016, in prep.) that diagnostic, correlatable fossil assemblages, including the *K. rostrata* Zone, would lie within the Normanville Group is supported by the results. Within the WANG section, the lower boundary of the *K. rostrata* Zone is defined at WANG/321.0, 83 m below the top of the section based on the occurrence of *Askepasma* sp. cf. *A. saproconcha*. A single specimen recovered from WANG/251.0, may also belong to *Askepasma* sp. cf. *A. saproconcha*, but due to its relatively poor preservation identification cannot be completely confirmed. If further sampling can replicate this occurrence then the base of the of the *K. rostrata* Zone could be pushed lower down within Sellick Hill Formation (Fig. 16, dotted line).

The base of the *K. rostrata* Zone at WANG/321.0 is further supported by presence of the camenellan tommotiid taxa *D. ajax* and *D. bacata* from WANG/321.0 to the top of the section. These species are key supplementary taxa in the *K. rostrata* Zone and so provide good independent support for the definition of this Zone in the upper part of the Sellick Hill Formation. The presence of *S. imbricata* (Fig. 20), previously associated with Facies Association D (Gravestock *et al.* 2001) and the *K. rostrata* Zone (Betts *et al.* 2016) is confirmed and the range of this taxon occurs in Facies Associations D and E from WANG/321.0 to WANG/350.0 in the section. Other taxa occurring within the *K. rostrata* Zone include chancelloriids (*Archiasterella* sp.), the hyolithid *Cupitheca* sp. and palmate, cultrate and siculate sclerites of *Australohalkieria parva*. Based on previous unpublished work by T. Brougham (unpub. Honours thesis, Macquarie University, 2009), the upper boundary of the *K. rostrata* Zone probably occurs high in the overlying Fork Tree Limestone, but the lack of taxa representing the succeeding *Micrina etheridgei* Zone (including *in situ* representatives of the eponym – see Betts *et al.* 2016) means the top of the *K. rostrata* (and concordant base of the *M. etheridgei* Zone) occurs at a stratigraphic level considerably above the top of the WANG section.

5.a.2. Chemostratigraphy

The negative excursion revealed within the WANG section between WANG/184.0 and WANG/307.0 in Facies Association C of the Sellick Hill Formation is interpreted to correspond to the SHICE $\delta^{13}C$ negative of the global chemostratigraphic curve, as identified in China based on $\delta^{13}C$ values of -2.0‰ and -4.0‰, with spikes to -6.0‰ (Zhu *et al.* 2006). Within the WANG section, the excursion consists of three peaks, with the second being the most negative by a considerable amount (-7.43‰ at WANG/215.0 as opposed to -4.96‰, the next highest peak at WANG/283.0). This result is uncharacteristic of the rest of the excursion as it is a very large spike on both sides of the peak. This could be an area of significant diagenesis, a possibility which is supported by analysis of the oxygen-isotope curve. Oxygen-isotope curves can be used to help identify diagenesis within samples, where they exhibit sharp positive spikes simultaneously with sharp negative spikes in the carbon-isotope curve (Melim *et al.* 2001). As the curves clearly exhibit this phenomenon at this level, it is reasonable to conclude diagenesis may be manifest.

In addition, Facies Association C of the Sellick Hill Formation contains multiple phosphatic hardground surfaces (Fig. 6; Mount & Kidder 1993), and these sediment-starved omission surfaces are well known to promote sharp negative swings in $\delta^{13}C$ (Bradbury *et al.* 2015). If this large peak period is removed from the WANG section chemostratigraphic curve, the first and third peaks

bracketing the uncharacteristic spike (WANG/195.0 and WANG/283.0, respectively) have $\delta^{13}C$ values ~-4.5‰, thus keeping the range within that of the global SHICE $\delta^{13}C$ negative, and allowing the SHICE $\delta^{13}C$ negative within the Normanville Group to lie within Facies Association C of the Sellick Hill Formation (Fig. 23). The work of Betts *et al.* (in prep.) recovered the SHICE $\delta^{13}C$ negative signal within the BHG, MORO and WAR sections of the Arrowie Basin, as well as the SHL section of the eastern Stansbury Basin. The chemostratigraphic data of the WANG section reconfirms the negative $\delta^{13}C$ trend expressed by the Arrowie Basin sections of Betts *et al.* (in prep.), and the WANG section provides a more complete SHICE $\delta^{13}C$ negative excursion (Fig. 24).

Stratigraphically down section, below the SHICE peak, the $\delta^{13}C$ curve trends as a large positive $\delta^{13}C$ peak identified within Facies Association A of the Sellick Hill Formation (WANG/120.0, Fig. 23). This peak has a maximum $\delta^{13}C$ value of 5.70‰ which is interpreted to correspond to the large global carbon-isotope chemostratigraphic spike of the ZHUCE $\delta^{13}C$ positive, which has been recorded with values around 6‰ and up to 7‰ (Knoll *et al.* 1995, Kouchinsky *et al.* 2001, Maloof *et al.* 2005, Li *et al.* 2009). This positive excursion within the WANG section aligns very well with the global chemostratigraphic curve (Fig. 24), further confirming the ZHUCE $\delta^{13}C$ positive event within the lower Normanville Group of the eastern Stansbury Basin.

Discovery of the ZHUCE $\delta^{13}C$ positive event in the lower Normanville Group represents the first report of this important carbon isotopic excursion from an Australian carbonate package, and has significant implications for the global chronostratigraphic timescale. Landing & Kouchinsky (2016) have indicated that the lower boundary of Cambrian Stage 2 should be placed at a stratigraphic level representing the first appearance of the micromolluscs *W. crosbyi* and *A. attleborensis*, and the *Skiagia ornata-Fimbrioglomerella membranacea* acritarch 'zone' **below** the ZHUCE $\delta^{13}C$ positive event. The first appearance of *W. crosbyi* as well as the genus *Aldanella* (represented by *Aldanella* sp. cf. *golubevi*) in Australia has been demonstrated to occur within the upper member of the Mount Terrible Formation underlying the Wangkonda Formation (Jacquet *et al.* in press; Fig. 24). This level occurs some 140 m below the ZHUCE $\delta^{13}C$ positive peak within Facies Association A of the Sellick Hill Formation, which potentially means this level could align with the proposed lower boundary of Cambrian Stage 2 of Landing & Kouchinsky (2016).

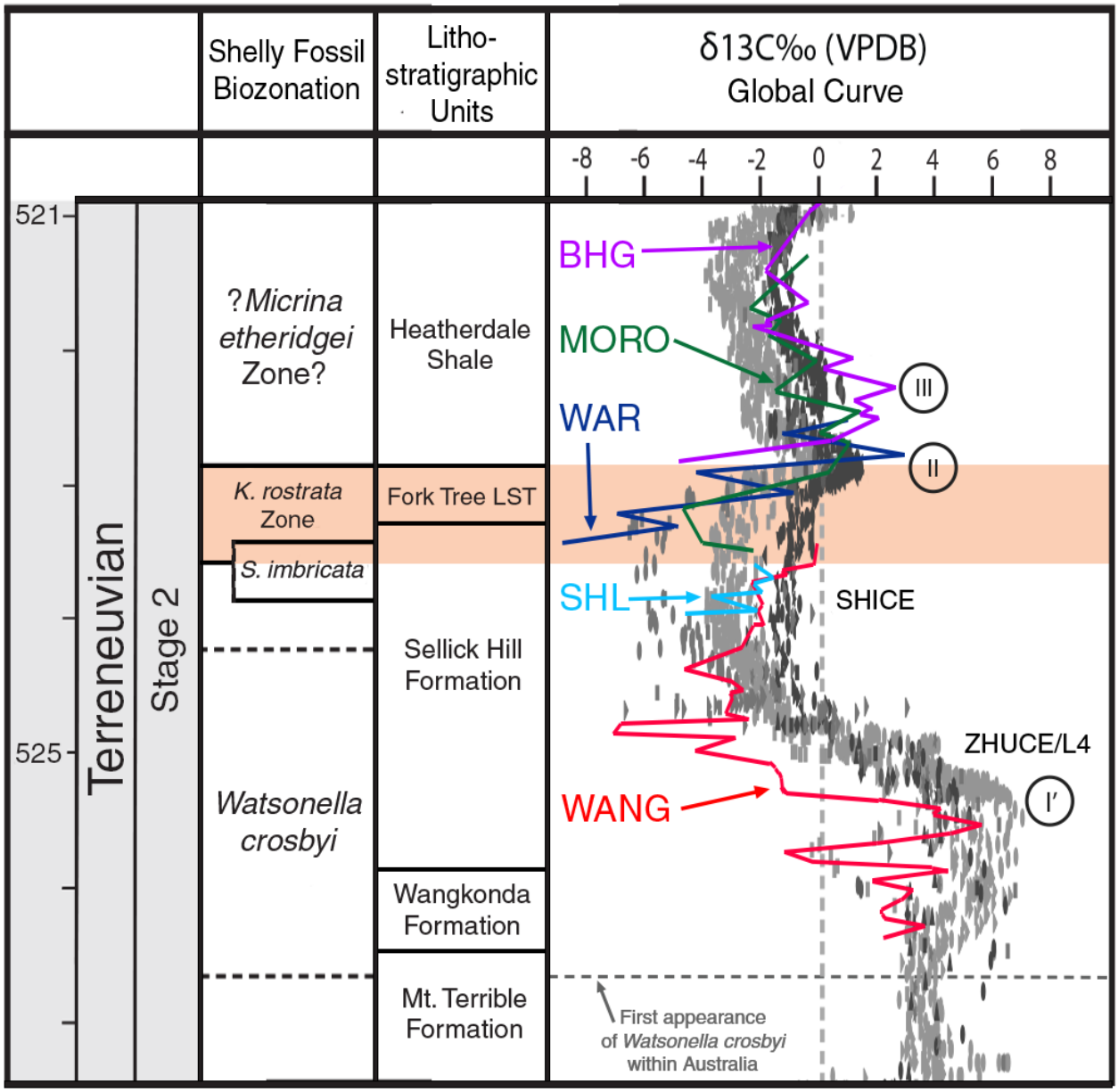

Figure 24. Correlation of the lower Cambrian Normanville Group (WANG from this study, SHL from Betts *et al.* in prep.) and the Arrowie Basin (MORO, BHG, WAR from Betts *et al.* in prep.) with the global chemostratigraphic curve. Biozones and lithostratigraphic units of the Normanville Group on the left. Orange box = *K. rostrata* Zone. Modified from Jacquet *et al.* (in press).

5.b. Regional chronostratigraphy

The paucity of fossil material from the lower half of the WANG section makes biostratigraphic correlation on fossil data alone difficult, and no other Australian lower Cambrian Basin has had chemostratigraphic analysis performed on rocks of synchronous age, making chemostratigraphic regional correlation of the lower half of the WANG section impossible. Thus, biostratigraphic correlation of the Wangkonda Formation and lower Sellick Hill Formation in the WANG section comes from the relative stratigraphic position of the section to the underlying

Mount Terrible and upper Sellick Hill Formations which bracket it, as well as the fossils reported from previous works (Jacquet *et al.* in press; Gravestock *et al.* 2001). The age of the lower Normanville Group when determined using fossil data has long been contentious, especially in relation to other South Australian strata. For example, the Mount Terrible Formation was claimed as equivalent to the Uratanna Formation of the Arrowie Basin (Daily 1973) and the Winulta Formation of the Yorke Peninsula, Stansbury Basin (Daily 1990), however this was based on chancelloriids and hyoliths which have long ranges and thus do not provide robust evidence. Acritarchs have been used to correlate the Yorke Peninsula of the western Stansbury Basin with the Arrowie Basin (Zang *et al.* 2007), but the Fleurieu Peninsula of the eastern Stansbury Basin received minimal attention, with most information coming solely from weathered outcrops. The Mount Terrible Formation revealed some poorly preserved acritarchs, however these were unable to be classified into any of the seven acritarch assemblages (Zang *et al.* 2007).

Trace fossils provide good information however, especially the vertical burrows of the ichnotaxon *Diplocraterion parallelum* identified from previous studies (Gravestock & Shergold 2001), which allows correlation of the Wangkonda Formation of the Normanville Group with the Parachilna Formation in the Arrowie Basin (Gravestock & Shergold 2001, Mángano & Buatois 2014) and the Winulta Formation on the Yorke Peninsula, western Stansbury Basin (Daily 1973) indicating a lower Cambrian, Terreneuvian Series, Stage 2 age.

5.b.1. Arrowie Basin

Betts *et al.* (2016) aligned the base of the *K. rostrata* Zone concurrent with the Hideaway Well Member of the Wilkawillina Limestone, through an interval to a level located just above the base of the overlying Winnitinny Creek Member (Fig. 25). The alignment of the top 83 m of the WANG section with the *K. rostrata* Zone of the Arrowie Basin makes this top section concurrent with the Hideaway Well Member of the Wilkawillina Limestone within the Hawker Group. The *K. rostrata* Zone has particular regional significance to this study as previous sections SHL and FTL (T. Brougham, unpub. Honours thesis, Macquarie University, 2009; Skovsted *et al.* 2015; Betts *et al.* in prep.) identified assemblages within the upper Normanville Group (upper Sellick Hill Formation, Fork Tree Limestone and Heatherdale Shale) containing diagnostic elements of the *K. rostrata* Zone, providing a secure regional correlation between the Arrowie and eastern Stansbury Basins.

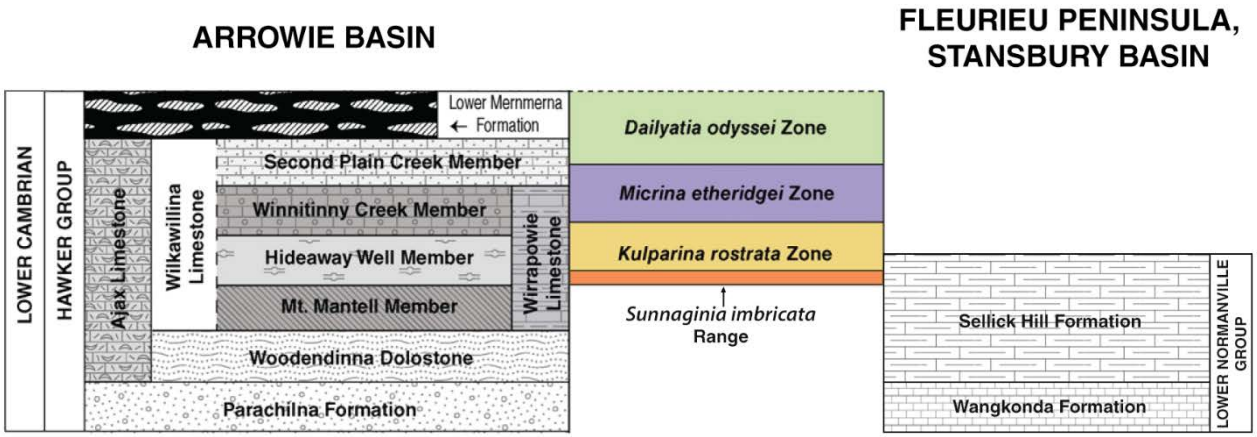

Figure 25. The Hawker Group of the Arrowie Basin at the left, new biozones coloured in the centre and the lower Normanville Group of the WANG section at the right. Modified from Betts *et al.* (2016).

The camenellan tommotiid *S. imbricata* occurs over a 37 m interval (WANG/321.0-358.0) with the first occurrence at the same stratigraphic level as *Askepasma* sp. cf. *A. saproconcha* and *D. ajax*, implying that the range of *S. imbricata* overlaps with the basal part of the *K. rostrata* Zone (Fig. 16, in *4.b. Biostratigraphic results* above). *S. imbricata* has a wide global distribution, and has been used as an important tie point in Cambrian Stage 2 strata. In Australia, the taxon is limited to the upper Sellick Hill Formation and it has not previously been recovered from the Hawker Group within the Arrowie Basin (Jacquet *et al.* in press). The overlapping range of *S. imbricata* with the lower *K. rostrata* Zone within the WANG section confirms a similar stratigraphic range of this taxon in the FTL section at Myponga Beach (T. Brougham, unpub. Honours thesis, Macquarie University, 2009; Skovsted *et al.* 2015) which was also attributed to the *K. rostrata* Zone. The lack of any fossil material typical of the zones younger than the *K. rostrata* Zone in concert with an abundance of *D. ajax* implies that the top 83 m of the WANG section can be confidently attributed to the *K. rostrata* Zone, helping to further reinforce correlation between the lower Cambrian Normanville Group succession with the Hawker Group of the Arrowie Basin.

Further evidence comes from the chemostratigraphic results. In all sections analysed by Betts *et al.* (in prep.), the SHICE $\delta^{13}C$ negative peak lay below the base of the *K. rostrata* Zone. Within the WANG section the same feature is apparent, with the base of the *K. rostrata* Zone located 83 m below the top of the section (WANG/321.0) and the SHICE $\delta^{13}C$ negative excursion peaking between 121 m and 209 m below the top of the section (WANG/283.0 and 195.0, respectively). Thus by means of a multi-proxy approach, the lower Cambrian carbonate rocks from the top of the WANG section in the Fleurieu Peninsula, eastern Stansbury Basin have been successfully aligned with the oldest successions of the Arrowie Basin.

5.b.2. Yorke Peninsula, western Stansbury Basin

Correlations between Normanville Group rocks of the eastern Stansbury Basin and the Yorke Peninsula of the western Stansbury Basin are difficult to determine on fossil data alone due to the largely unfossiliferous nature of lowermost units on the Yorke Peninsula, as well as the lack of studies on the area (Paterson *et al.* 2007). The focus of this study was on shelly fossils, whereas most previous studies of the Yorke Peninsula primarily used archaeocyathids to form their zonation (Zhuravlev & Gravestock 1994, Gravestock *et al.* 2001), none of which were recovered from the WANG section. The chemostratigraphic results do reveal a relationship between the Yorke and Fleurieu Peninsulas, as previous chemostratigraphic data from the Stansbury West-1 drill core (P. A. Hall, unpub. PhD Thesis, University of Adelaide, 2012) record a negative $\delta^{13}C$ excursion within the Kulpara Limestone with values down to -2.80‰ $\delta^{13}C$, potentially corresponding to the SHICE $\delta^{13}C$ negative event.

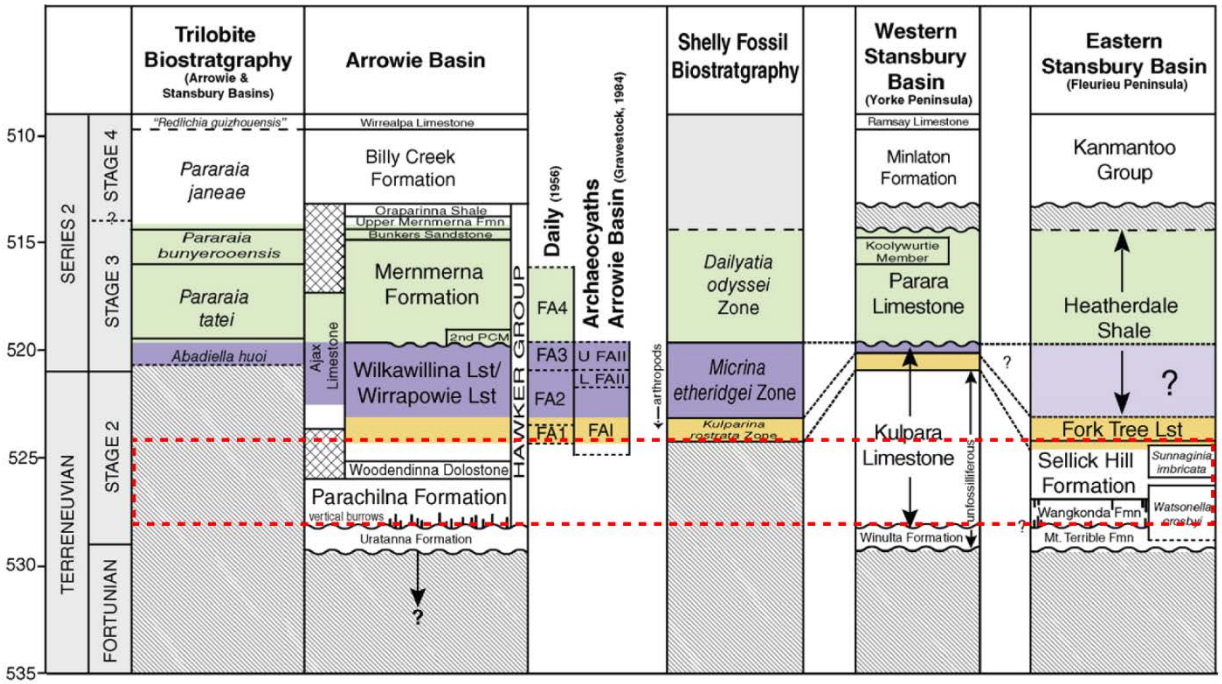

Figure 26. Regional correlation of South Australia, with included trilobite, archaeocyathid and shelly fossil Zones. The WANG section (lower Normanville Group) is boxed in red. Modified from Betts *et al.* (2016).

In summary, trace fossil data from the Wangkonda Formation and relatively diverse shelly fossil faunas from the Sellick Hill Formation (especially the upper part) and a now complete chemostratigraphic curve through the lower Normanville Group indicates the Wangkonda-Sellick Hill Formation succession lies entirely within the Terreneuvian Series, unnamed Cambrian Stage 2. Trace fossil data, especially the presence of the vertical burrows of *Diplocraterion* from the Wangkonda Formation (Gravestock & Shergold 2001, Jacquet *et al.* in press) and the horizontal burrows of *Treptichnus* isp. in the lower Sellick Hill Formation suggest the Wangkonda-Sellick Hill

succession can be aligned with the Parachilna Formation through to the Hideaway Well Member of the Wilkawillina Limestone and concurrent Wirrapowie Limestone (lower Hawker Group) of the Arrowie Basin. The succession is also associated with the upper Winulta Formation through to the top of the Kulpara Formation of the Yorke Peninsula, western Stansbury Basin (Fig. 26).

5.c. Global chronostratigraphy

High levels of regional endemism and facies dependence hinders accurate global correlation of the lower Cambrian timescale using shelly fossil data alone (Landing 1994, Landing *et al.* 2013). This makes many of the fossils recovered from the WANG section difficult to use for global correlation, for example the abundant *D. ajax* which is endemic to East Gondwana (Bischoff 1976, Skovsted *et al.* 2015). However, independent chemostratigraphic data, when combined with synchronous regional biostratigraphic schemes, provides a more accurate and robust means of constraining and defining lower Cambrian chronostratigraphy.

The lower half of the WANG section contains no fossils which can be accurately correlated globally, however *W. crosbyi* has been discovered in previous studies (Alexander & Gravestock 1990, Gravestock *et al.* 2001, Jacquet *et al.* in press) and ranges from the upper member of the Mount Terrible Formation through to the Sellick Hill Formation Facies Association C (Gravestock *et al.* 2001). The record of *W. crosbyi* from Facies Association C of the Sellick Hill Formation at Myponga Beach, reported by Gravestock *et al.* (2001), has yet to be independently replicated by more recent studies (T. Brougham, unpub. Honours thesis, Macquarie University, 2009; Skovsted 2015 and herein). The Arrowie Basin has not revealed any specimens of *W. crosbyi,* likely due to the hostile, supratidal depositional environment of the Woodendinna Dolostone and Mount Mantell Member of the Wilkawillina Limestone and the siliciclastic nature of the underlying Parachilna Formation which correlate with the WANG section reported here (Fig. 26). This essentially means that the lower Normanville rocks are the only strata yielding *W. crosbyi* in South Australia. This taxon has been recorded from South China, Siberia, Morocco and Avalonia (Steiner *et al.* 2007, Kouchinsky *et al.* 2012, Devaere *et al.* 2013, Landing *et al.* 2013), all with first occurrences in Cambrian Stage 2.

The first appearance of *W. crosbyi* within these palaeocontinents has been consistently revised to the late Nemakit-Daldynian and early Tommotian Stages of Siberia, equivalent to the early-middle Terreneuvian Series, Stage 2, based on the addition of independent isotopic chemostratigraphic data (e.g. Nagovitsin *et al*. 2015; Landing & Kouchinsky 2016). The addition of chemostratigraphic data has allowed further progress to be made on defining the first appearance of

this taxon, including its potential use as the index fossil to define the lower boundary of Cambrian Stage 2 (Landing & Kouchinsky 2016). The ZHUCE $\delta^{13}C$ positive is identified within Facies Association A of the Sellick Hill Formation, with a value of 5.70‰ at WANG/120.0, corresponding to global values (Knoll *et al.* 1995, Kouchinsky *et al.* 2001, Maloof *et al.* 2005, Li *et al.* 2009). Although the range of *W. crosbyi* in Australia, South China, Siberia and Avalonia have a considerable overlap in ranges (Fig. 27), it is the first appearance of *W. crosbyi* at stratigraphic levels in the Mount Terrible Formation (Jacquet *et al.* in press) below the ZHUCE $\delta^{13}C$ peak identified in the WANG section which indicates the base of Cambrian Stage 2 can potentially be identified in Australia and allow correlation with this level in other Cambrian palaeocontinents.

The upper half of the WANG section has a diverse range of shelly fossil taxa, most being endemic to East Gondwana with the exception of *S. imbricata*. This taxon had a wide distribution in the early Cambrian period, having been recovered from South Australia, Avalonia (North America and England), the Siberian Platform, Morocco and Mongolia (Murdock *et al.* 2012). These occurrences all correspond broadly to the Tommotian Stage of Siberia, primarily due to fossils recovered from Avalonia (North America, Landing 1988; Newfoundland, Landing *et al.* 1989) and the definition of a *S. imbricata* biozone erected within the Bonavista Group (Fig. 27). This would potentially correlate the top of the WANG section with the lower Bonavista Group of Avalonia and the upper *N. sunnaginicus* Zone of Siberia, within the Tommotian Stage of the Terreneuvian Series, Stage 2.

The primary global correlation arises from the chemostratigraphic data, in particular the SHICE $\delta^{13}C$ negative. In Avalonia, *S. imbricata* occurs with the lower Bonavista Group (Landing *et al.* 1989; Fig. 27), which extends above the SHICE $\delta^{13}C$ negative excursion. Within the WANG section, *S. imbricata* was recovered from horizons above the SHICE $\delta^{13}C$ peak, thus allowing correlation both with biostratigraphic fossil data and chemostratigraphic carbon-isotope trends.

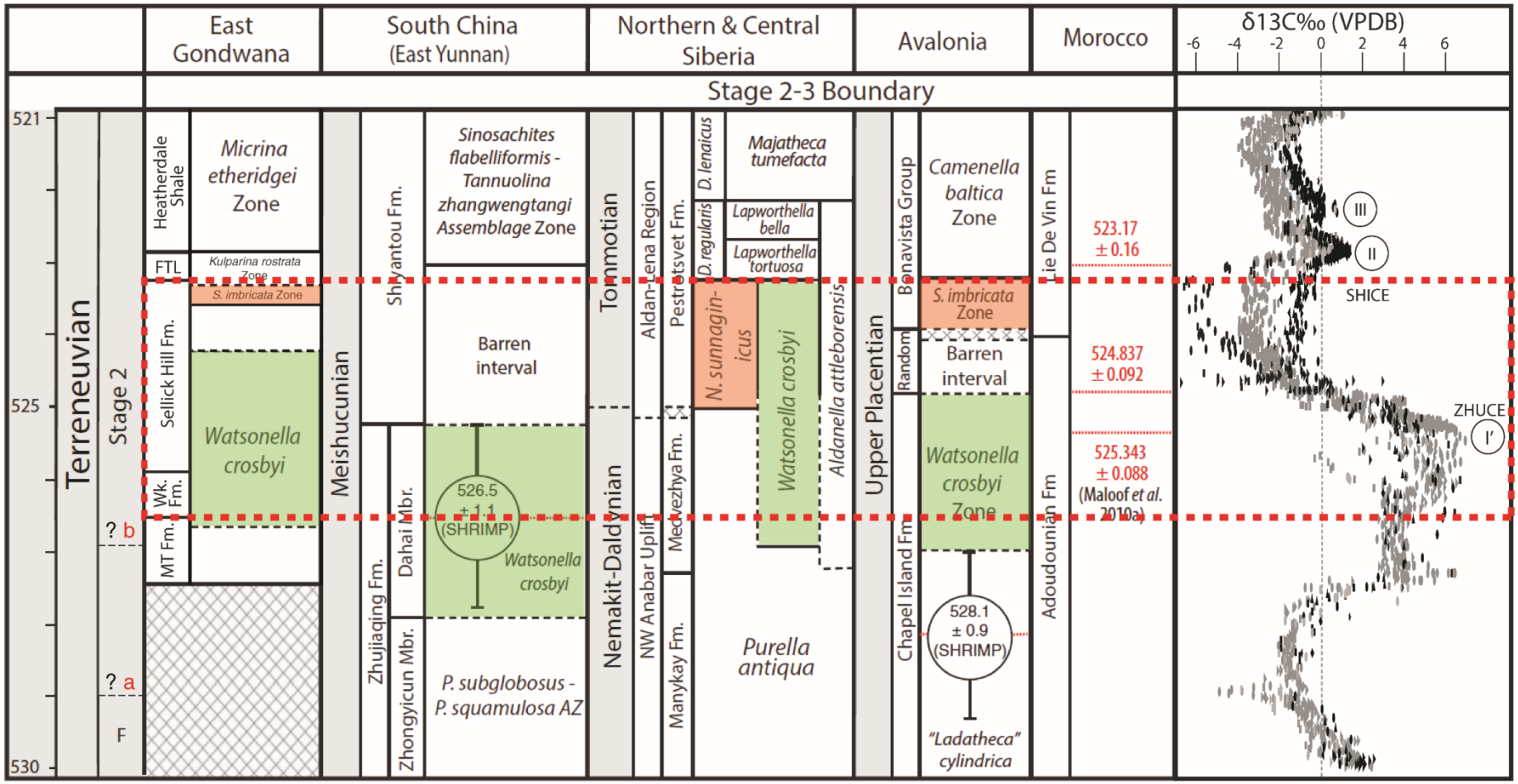

Figure 27. Global correlation of the biozones from the WANG section (within the dotted box) and biozones from other palaeocontinents. *Sunnaginia imbricata* range and contemporaries in orange, *Watsonella crosbyi* range and contemporaries in green. Previous Terreneuvian Series, Stage 2 lower boundary estimate indicated by the red 'a'. Potential new boundary indicated by the red 'b'. Modified from Jacquet *et al.* (in press).

6. Conclusions

Betts *et al*. (2016, in prep.) predicted that correlatable regional biostratigraphic fossil assemblages of the Arrowie Basin would overlap to some extent with carbonate packages of the upper Normanville Group of the eastern Stansbury Basin, allowing these two basins to be aligned on a regional level. They further indicated that the poorly sampled carbonates of the lower Normanville Group should be older than the Hawker Group package in the Arrowie Basin and predicted that the globally recognised ZHUCE $\delta^{13}C$ positive would lie within the Normanville Group. The ZHUCE $\delta^{13}C$ positive is associated with the base of Terreneuvian Series, Stage 2 (Landing and Kouchinsky 2016), so this boundary could potentially be identified within the Normanville Group. To this end, the aims of this study were to use multi-proxy (biostratigraphic and chemostratigraphic) methods to ascertain the predictive effectiveness of these techniques when used as independent, synchronous data sets.

Aim 1: To use biostratigraphic and chemostratigraphic proxy data to resolve the age of the lower Cambrian Normanville Group.

Outcome: The multi-proxy methodology used in this study was very effective. The lowest biozone of the Arrowie Basin, the *K. rostrata* Zone, aligns with the top 83 m of the upper Sellick Hill Formation in the WANG section, based on co-occurrence of key taxa including *Askepasma* sp. cf. *A. saproconcha* and three supplementary taxa, *D. ajax*, *D. bacata* and *S. imbricata*. The chemostratigraphic curve for the WANG section captures carbon- and oxygen-isotope excursions that closely match the global chemostratigraphic scheme, providing clear evidence that the lower Normanville Group rocks are Cambrian Stage 2 in age.

Aim 2: To determine whether the ZHUCE $\delta^{13}C$ positive event lies within the Normanville Group.

Outcome: The ZHUCE $\delta^{13}C$ positive event is identified for the first time in Australia within Facies Association A of the Sellick Hill Formation (WANG/120.0), at a stratigraphic level predicted by the previous multi-proxy work of Betts *et al.* (2016). In addition, the SHICE $\delta^{13}C$ negative event peaks within Facies Association C of the Sellick Hill Formation in the WANG section below the incoming of the *K. rostrata* Zone providing direct correlation with this level in the Arrowie Basin (Betts *et al.* 2016).

Aim 3: To determine whether the lower boundary of the Terreneuvian Series, Stage 2 of the International Cambrian timescale can be identified within the Normanville Group.

Outcome: Identification of the first occurrence of the widespread micromolluscan taxon *W. crosbyi* in the middle member of the Mount Terrible Formation (Jacquet *et al.* in press), 140 m **below** the peak of the ZHUCE $\delta^{13}C$ positive event (Fig. 27), strongly suggests that the lower boundary of Terreneuvian Series, Stage 2 can potentially be identified within the Normanville Group.

References

ABELE, C. & MCGOWRAN, B. 1959. The geology of the Cambrian south of Adelaide (Sellick Hill to Yankalilla). *Transactions of the Royal Society of South Australia* **82**, 301-20.

AHARON, P., SCHIDLOWSKI, M. & SINGH, I. B. 1987. Chronostratigraphic markers in the end-Precambrian carbon isotope record of the Lesser Himalaya. *Nature* **327**, 699-702.

ALEXANDER, E. M. & GRAVESTOCK, D. I. 1990. Sedimentary facies in the Sellick Hill Formation, Fleurieu Peninsula, South Australia. *Geological Society of Australia, Special Publication* **16**, 269-89.

BABCOCK, L. E. & PENG, S. 2007. Cambrian chronostratigraphy: current state and future plans. *Palaeogeography, Palaeoclimatology, Palaeoecology* **254**(1), 62-66.

BABCOCK, L. E., PENG, S., GEYEF, G. & SHERGOLD, J. H. 2005. Changing perspectives on Cambrian chronostratigraphy and progress toward subdivision of the Cambrian System. *Geosciences Journal* **9**(2), 101-06.

BABCOCK, L. E., ROBISON, R. A., REES, M. N., PENG, S. & SALTZMAN, M. R. 2007. The global boundary stratotype section and point (GSSP) of the Drumian Stage (Cambrian) in the Drum Mountains, Utah, USA. *Episodes* **30**(2), 85.

BENGTSON, S., MORRIS, S. C., COOPER, B., JELL, P. & RUNNEGAR, B. N. 1990. Early Cambrian fossils from South Australia. *Memoirs of the Association of Australasian Palaeontologists* **9**, 1-364.

BETTS, M. J., TOPPER, T. P., VALENTINE, J. L., SKOVSTED, C. B., PATERSON, J. R. & BROCK, G. A. 2014. A new early Cambrian bradoriid (Arthropoda) assemblage from the northern Flinders Ranges, South Australia. *Gondwana Research* **25**(1), 420-37.

BETTS, M. J., BROCK, G. A., PATERSON, J. R., JAGO, J. B. & ANDREW, A. S. 2015. Integrated Shelly Fossil Biostratigraphy and Carbon and Oxygen Chemostratigraphy: Applying a Multi-Proxy Toolkit to Correlating the Lower Cambrian of South Australia. In *AAPG-SEG International Conference & Exhibition* Melbourne.

BETTS, M. J., PATERSON, J. R., JAGO, J. B., JACQUET, S. M., SKOVSTED, C. B., TOPPER, T. P. & BROCK, G. A. 2016. A new lower Cambrian shelly fossil biostratigraphy for South Australia. *Gondwana Research* **36**, 176-208.

BETTS, M. J., PATERSON, J. R., JAGO, J. B., JACQUET, S. M., SKOVSTED, C. B., TOPPER, T. P. & BROCK, G. A. (in review). Shelly fossils from the Dailyatia odyssei – Stoibostrombus crenulatus Assemblage Zone (Cambrian Series 2, Stages 3-4), Arrowie Basin, South Australia. *Gondwana Research*.

BETTS, M. J., BROCK, G. A., PATERSON, J. R., JAGO, J. B., ANDREW, A. S. & HALL, P. A. (in prep.). Integrated shelly fossil biostratigraphy and carbon isotope chemostratigraphy of the early Cambrian, South Australia. *Geology*.

BISCHOFF, G. 1976. Dailyatia, a new genus of the Tommotiidae from Cambrian strata of SE Australia (Crustacea, Cirripedia). *Senckenbergiana lethaea* **57**(1), 1-33.

BRADBURY, H. J., VANDEGINSTE, V. & JOHN, C. M. 2015. Diagenesis of phosphatic hardgrounds in the Monterey Formation: A perspective from bulk and clumped isotope geochemistry. *Geological Society of America Bulletin* **127**(9-10), 1453-63.

BRASIER, M. D. 1993. Towards a carbon isotope stratigraphy of the Cambrian System: potential of the Great Basin succession. *Geological Society, London, Special Publications* **70**(1), 341-50.

BRASIER, M. D., SHIELDS, G., KULESHOV, V. N. & ZHEGALLO, E. A. 1996. Integrated chemo-and biostratigraphic calibration of early animal evolution: Neoproterozoic–early Cambrian of southwest Mongolia. *Geological Magazine* **133**(04), 445-85.

BROCK, G. A., ENGELBRETSEN, M. J., JAGO, J. B., KRUSE, P. D., LAURIE, J. R., SHERGOLD, J. H., SHI, G. R. & SORAUF, J. E. 2000. Palaeobiogeographic affinities of Australian Cambrian faunas. *Memoir-Association of Australasian Palaeontologists* **23**, 1-62.

CLARKE, L. J. & JENKYNS, H. C. 1999. New oxygen isotope evidence for long-term Cretaceous climatic change in the Southern Hemisphere. *Geology* **27**(8), 699-702.

DAILY, B. 1956. The Cambrian in South Australia. In *El Sistema Cambrico, su Paleogeografia y el Problema de su Base. Report 20th International Geological Congress* (ed J. Rodgers). pp. 91-147. Mexico City.

DAILY, B. 1963. The Fossilferous Cambrian Succession on Fleurieu Peninsula, South Australia. *Records of the South Australian Museum* **14**, 579-602.

DAILY, B. 1969. Fossiliferous Cambrian sediments and low-grade metamorphics, Fleurieu Peninsula, South Australia. *Geological Excursions Handbook* **3**, 49-54.

DAILY, B. 1973. Discovery and significance of basal Cambrian Uratanna Formation, Mt. Scott Range, Flinders Ranges, South Australia. *Search* **4**(6), 202-05.

DAILY, B. 1976. The Cambrian of the Flinders Ranges. In *25th International Geological Congress, Excursion Guide* pp. 15-19. Sydney.

DAILY, B. 1990. Cambrian stratigraphy of Yorke Peninsula. *Geological Society of Australia, Special Publication* **16**, 215-29.

DAILY, B. & MILNES, A. R. 1973. Stratigraphy, structure and metamorphism of the Kanmantoo Group (Cambrian) in its type section east of Tunkalilla Beach, South Australia. *Transactions of the Royal Society of South Australia* **97**(3), 213-42.

DEBRENNE, F. & GRAVESTOCK, D. I. 1990. Archaeocyatha from the Sellick Hill Formation and Fork Tree Limestone on Fleurieu Peninsula, South Australia. In *The Evolution of a Late Precambrian-Early Palaeozoic Rift Complex: The Adelaide Geosyncline* (eds J. Jago and P. Moore). pp. 290-309. Geological Society of Australia, Special Publication no. 16.

DEVAERE, L., CLAUSEN, S., STEINER, M., ÁLVARO, J. J. & VACHARD, D. 2013. Chronostratigraphic and palaeogeographic significance of an early Cambrian microfauna from the Heraultia Limestone, northern Montagne Noire, France. *Palaeontologia Electronica* **16**(2), 17A-91.

DEVAERE, L., CLAUSEN, S., MONCERET, E., VIZCAÏNO, D., VACHARD, D. & GENGE, M. C. 2014. The tommotiid Kelanella and associated fauna from the early Cambrian of southern Montagne Noire (France): implications for camenellan phylogeny. *Palaeontology* **57**(5), 979-1002.

ERWIN, D. H. & VALENTINE, J. W. 2012. *The Cambrian explosion: the construction of animal biodiversity*. Greenwood, CO: Roberts Publishers.

ERWIN, D. H., LAFLAMME, M., TWEEDT, S. M., SPERLING, E. A., PISANI, D. & PETERSON, K. J. 2011. The Cambrian conundrum: early divergence and later ecological success in the early history of animals. *Science* **334**(6059), 1091-97.

ESAKOVA, N. V. & ZHEGALLO, E. A. 1996. Biostratigraphy and fauna of the lower Cambrian of Mongolia. *Trudy, Sovmestnaya Rossiysko-Mongol'skaya Paleontologicheskaya Ekspeditsiya* **46**, 214.

ETHERIDGE, R. 1890. On some Australian species of the family Archaeocyathinae. *Transactions of the Royal Society of South Australia* **13**, 10-22.

FAN, R., DENG, S. & ZHANG, X. 2011. Significant carbon isotope excursions in the Cambrian and their implications for global correlations. *Science China Earth Sciences* **54**(11), 1686-95.

FRICKE, H. C., CLYDE, W. C., O'NEIL, J. R. & GINGERICH, P. D. 1998. Evidence for rapid climate change in North America during the latest Paleocene thermal maximum: oxygen isotope compositions of biogenic phosphate from the Bighorn Basin (Wyoming). *Earth and Planetary Science Letters* **160**(1), 193-208.

GRABAU, A. W. 1900. Palaeontology of the Cambrian terranes of the Boston Basin. *Occasional Papers of the Boston Society of Natural History* **4**, 601-94.

GRAVESTOCK, D. I. & GATEHOUSE, C. G. 1995. Stansbury Basin. In *The Geology of South Australia* (eds J. Drexel and W. Preiss). pp. 5-19. Mines and Energy South Australia Bulletin 54.

GRAVESTOCK, D. I. & SHERGOLD, J. H. 2001. Australian Early and Middle Cambrian sequence biostratigraphy with implications for species diversity and correlation. In *Ecology of the Cambrian Radiation* (eds A. Y. Zhuravlev and R. Riding). pp. 107-36. New York: Columbia University Press.

GRAVESTOCK, D. I., ALEXANDER, E. M., DEMIDENKO, Y. E., ESAKOVA, N. V., HOLMER, L. E., JAGO, J. B., LIN, T.-R., MELNIKOVA, L. M., PARKHAEV, P. Y., ROZANOV, A. Y., USHATINSKAYA, G. T., ZANG, W.-L., ZHEGALLO, E. A. & ZHURAVLEV, A. Y. 2001. The Cambrian biostratigraphy of the Stansbury Basin, South Australia. *Transactions of the Palaeontological Institute of the Russian Academy of Sciences* **282**, 344.

HE, T., PEI, F. & FU, G. 1984. Some small shelly fossils from the Lower Cambrian Xinji Formation in Fangcheng County, Henan Province. *Acta Palaeontologica Sinica* **23**, 350-57.

HOWCHIN, W. 1897. On the Occurrence of Lower Cambrian Fossils in the Mount Lofty Ranges. *Transactions of the Royal Society of South Australia* **21**, 74-86.

ISHIKAWA, T., UENO, Y., SHU, D., LI, Y., HAN, J., GUO, J., YOSHIDA, N., MARUYAMA, S. & KOMIYA, T. 2014. The δ13C excursions spanning the Cambrian explosion to the Canglangpuian mass extinction in the Three Gorges area, South China. *Gondwana Research* **25**(3), 1045-56.

JACQUET, S. M., BROUGHAM, T., SKOVSTED, C. B., JAGO, J. B., LAURIE, J. R., BETTS, M. J., TOPPER, T. P. & BROCK, G. A. (in press). Watsonella crosbyi from the lower Cambrian (Terreneuvian, Stage 2) Mount Terrible Formation in South Australia. *Geological Magazine*.

JAGO, J. B. & GATEHOUSE, C. G. 2007. Early Cambrian trace fossils from the Kanmantoo Group at Red Creek, South Australia, and their stratigraphic significance. *Australian Journal of Earth Sciences* **54**(4), 531-40.

JAGO, J. B., GEHLING, J. G., PATERSON, J. R., BROCK, G. A. & ZANG, W. 2012. Cambrian stratigraphy and biostratigraphy of the Flinders Ranges and the north coast of Kangaroo Island, South Australia. *Episodes* **35**(1), 247-55.

JENKINS, R. J. F., COOPER, J. A. & COMPSTON, W. 2002. Age and biostratigraphy of Early Cambrian tuffs from SE Australia and southern China. *Journal of the Geological Society* **159**(6), 645-58.

JEPPSSON, L., ANEHUS, R. & FREDHOLM, D. 1999. The optimal acetate buffered acetic acid technique for extracting phosphatic fossils. *Journal of Paleontology* **73**(5), 964-72.

JOHNSEN, S. J., DAHL-JENSEN, D., GUNDESTRUP, N., STEFFENSEN, J. P., CLAUSEN, H. B., MILLER, H., MASSON-DELMOTTE, V., SVEINBJÖRNSDOTTIR, A. E. & WHITE, J. 2001. Oxygen isotope and palaeotemperature records from six Greenland ice-core stations: Camp Century, Dye-3, GRIP, GISP2, Renland and NorthGRIP. *Journal of Quaternary Science* **16**(4), 299-307.

KAUFMAN, A. J. & KNOLL, A. H. 1995. Neoproterozoic variations in the C-isotopic composition of seawater: stratigraphic and biogeochemical implications. *Precambrian Research* **73**(1), 27-49.

KNOLL, A. H., KAUFMAN, A. J., SEMIKHATOV, M. A., GROTZINGER, J. P. & ADAMS, W. 1995. Sizing up the sub-Tommotian unconformity in Siberia. *Geology* **23**(12), 1139-43.

KOUCHINSKY, A., BENGTSON, S., MISSARZHEVSKY, V., PELECHATY, S., TORSSANDER, P. & VAL'KOV, A. 2001. Carbon isotope stratigraphy and the problem of a pre-Tommotian Stage in Siberia. *Geological Magazine* **138**(04), 387-96.

KOUCHINSKY, A., BENGTSON, S., RUNNEGAR, B., SKOVSTED, C., STEINER, M. & VENDRASCO, M. 2012. Chronology of early Cambrian biomineralization. *Geological Magazine* **149**(2), 221.

LANDING, E. 1988. Lower Cambrian of eastern Massachusetts: stratigraphy and small shelly fossils. *Journal of Paleontology* **62**(05), 661-95.

LANDING, E. 1994. Precambrian-Cambrian boundary global stratotype ratified and a new perspective of Cambrian time. *Geology* **22**(2), 179-82.

LANDING, E. & GEYER, G. 2012. Misplaced faith–limitations of the first appearance datum (FAD) in chronostratigraphy and proposal of more robust Lower Cambrian correlation standards. *Journal of Guizhou University (Natural Science) 29 (supplement)*, 170-71.

LANDING, E. & KOUCHINSKY, A. 2016. Correlation of the Cambrian Evolutionary Radiation: geochronology, evolutionary stasis of earliest Cambrian (Terreneuvian) small shelly fossil (SSF) taxa, and chronostratigraphic significance. *Geological Magazine* **153**(4), 750-56.

LANDING, E., MYROW, P., BENUS, A. P. & NARBONNE, G. M. 1989. The Placentian Series: appearance of the oldest skeletalized faunas in southeastern Newfoundland. *Journal of Paleontology* **63**(06), 739-69.

LANDING, E., GEYER, G., BRASIER, M. D. & BOWRING, S. A. 2013. Cambrian evolutionary radiation: context, correlation, and chronostratigraphy—overcoming deficiencies of the first appearance datum (FAD) concept. *Earth-Science Reviews* **123**, 133-72.

LARSSON, C. M., SKOVSTED, C. B., BROCK, G. A., BALTHASAR, U., TOPPER, T. P., HOLMER, L. E. & LANE, P. 2014. Paterimitra pyramidalisfrom South Australia: scleritome, shell structure and evolution of a lower Cambrian stem group brachiopod. *Palaeontology* **57**(2), 417-46.

LI, G., ZHAO, X., GUBANOV, A., ZHU, M. & NA, L. 2011. Early Cambrian mollusc Watsonella crosbyi: a potential GSSP index fossil for the base of the Cambrian Stage 2. *Acta Geologica Sinica (English Edition)* **85**(2), 309-19.

LI, D. A., LING, H.-F., JIANG, S.-Y., PAN, J.-Y., CHEN, Y.-Q., CAI, Y.-F. & FENG, H.-Z. 2009. New carbon isotope stratigraphy of the Ediacaran–Cambrian boundary interval from SW China: implications for global correlation. *Geological Magazine* **146**(04), 465-84.

MADIGAN, C. T. 1925. The geology of the Fleurieu Peninsula. Part 1—The coast from Sellick's Hill to Victor Harbor. *Transactions of the Royal Society of South Australia* **49**, 198-212.

MADIGAN, C. T. 1927. The geology of the Willunga Scarp. *Transactions of the Royal Society of South Australia* **51**, 398-409.

MALOOF, A. C., SCHRAG, D. P., CROWLEY, J. L. & BOWRING, S. A. 2005. An expanded record of Early Cambrian carbon cycling from the Anti-Atlas Margin, Morocco. *Canadian Journal of Earth Sciences* **42**(12), 2195-216.

MALOOF, A. C., PORTER, S. M., MOORE, J. L., DUDAS, F. O., BOWRING, S. A., HIGGINS, J. A., FIKE, D. A. & EDDY, M. P. 2010*a*. The earliest Cambrian record of animals and ocean geochemical change. *Geological Society of America Bulletin* **122**(11-12), 1731-74.

MALOOF, A. C., RAMEZANI, J., BOWRING, S. A., FIKE, D. A., PORTER, S. M. & MAZOUAD, M. 2010*b*. Constraints on early Cambrian carbon cycling from the duration of the Nemakit-Daldynian-Tommotian boundary 13C shift, Morocco. *Geology* **38**(7), 623-26.

MÁNGANO, M. G. & BUATOIS, L. A. 2014. Decoupling of body-plan diversification and ecological structuring during the Ediacaran–Cambrian transition: evolutionary and geobiological feedbacks. *Proceedings of the Royal Society of London B: Biological Sciences* **281**, 1-9.

MARSHALL, J. D. 1992. Climatic and oceanographic isotopic signals from the carbonate rock record and their preservation. *Geological Magazine* **129**(2), 143-60.

MARSHALL, C. R. 2006. Explaining the Cambrian "explosion" of animals. *Annu. Rev. Earth Planet. Sci.* **34**, 355-84.

MATTHEWS, S. C. & MISSARZHEVSKY, V. 1975. Small shelly fossils of late Precambrian and early Cambrian age: a review of recent work. *Journal of the Geological Society* **131**(3), 289-303.

MELIM, L. A., SWART, P. K. & MALIVA, R. G. 2001. Meteoric and marine-burial diagenesis in the subsurface of Great Bahama Bank. In *Subsurface Geology of a Prograding Carbonate Platform Margin, Great Bahama Bank* (ed G. R. N). pp. 137-62. SEPM Special Publication.

MIALL, A. D. 2015. Updating uniformitarianism: stratigraphy as just a set of 'frozen accidents'. *Geological Society, London, Special Publications* **404**(1), 11-36.

MISSARZHEVSKY, V. V. & MAMBETOV, A. M. 1981. Stratigraphy and fauna of Cambrian and Precambrian boundary beds of Maly Karatau. *Trudy Akademii Nauka SSSR, Moscow* **326**, 1-90.

MOUNT, J. F. & KIDDER, D. 1993. Combined flow origin of edgewise intraclast conglomerates: Sellick Hill Formation (Lower Cambrian), South Australia. *Sedimentology* **40**(2), 315-29.

MURDOCK, D. J. E., DONOGHUE, P. C. J., BENGTSON, S. & MARONE, F. 2012. Ontogeny and microstructure of the enigmatic Cambrian tommotiid Sunnaginia Missarzhevsky, 1969. *Palaeontology* **55**(3), 661-76.

NAGOVITSIN, K. E., ROGOV, V. I., MARUSIN, V. V., KARLOVA, G. A., KOLESNIKOV, A. V., BYKOVA, N. V. & GRAZHDANKIN, D. V. 2015. Revised Neoproterozoic and Terreneuvian stratigraphy of the Lena-Anabar Basin and north-western slope of the Olenek Uplift, Siberian Platform. *Precambrian Research* **270**, 226-45.

PARKHAEV, P. Y. 2001. Molluscs and siphonoconchs. *The Cambrian biostratigraphy of the Stansbury basin, South Australia. Transactions of the Russian Acadademy of Sciences* **282**, 133-203.

PARKHAEV, P. Y. & KARLOVA, G. 2011. Taxonomic revision and evolution of Cambrian mollusks of the genus Aldanella Vostokova, 1962 (Gastropoda: Archaeobranchia). *Paleontological Journal* **45**(10), 1145-205.

PATERSON, J. R., SKOVSTED, C. B., BROCK, G. A. & JAGO, J. B. 2007. An early Cambrian faunule from the Koolywurtie Limestone Member (Parara Limestone), Yorke Peninsula, South Australia and its biostratigraphic significance. *Australasian Palaeontological Memoirs* **34**, 131-46.

PENG, S. & BABCOCK, L. E. 2011. Continuing progress on chronostratigraphic subdivision of the Cambrian System. *Bulletin of Geosciences* **86**(3), 391-96.

PENG, S., BABCOCK, L., ROBISON, R., LIN, H., REES, M. & SALTZMAN, M. 2004. Global Standard Stratotype-section and Point (GSSP) of the Furongian Series and Paibian Stage (Cambrian). *Lethaia* **37**(4), 365-79.

PENG, S., BABCOCK, L. E., ZUO, J., LIN, H., ZHU, X., YANG, X., ROBISON, R. A., QI, Y., BAGNOLI, G. & CHEN, Y. a. 2009. The global boundary stratotype section and point (GSSP) of the Guzhangian Stage (Cambrian) in the Wuling Mountains, northwestern Hunan, China. *Episodes* **32**(1), 41-55.

PENG, S., BABCOCK, L. E. & COOPER, R. A. 2012*a*. The Cambrian Period. In *The Geologic Time Scale 2012 2-Volume Set. Volume 2* (eds F. M. Gradstein, J. G. Ogg, M. Schmitz and G. Ogg). pp. 437-88. Amsterdam: Elsevier.

PENG, S., BABCOCK, L. E., ZUO, J., ZHU, X., LIN, H., YANG, X., QI, Y., BAGNOLI, G. & WANG, L. 2012*b*. Global standard stratotype-section and point (GSSP) for the base of the Jiangshanian Stage (Cambrian: Furongian) at Duibian, Jiangshan, Zhejiang, southeast China. *Episodes* **35**(4), 462-77.

ROZANOV, A. Y., MISSARZHEVSKY, V., VOLKOVA, N., VORONOVA, L., KRYLOV, I., KELLER, B., KOROLYUK, I., LENDZION, K., MICHNIAK, R. & PYKHOVA, N. 1969. The Tommotian Stage and the Cambrian lower boundary problem. *Transactions of the Academy of Sciences of the USSR Nauka* **206**, 1-380.

SALTZMAN, M. R., COWAN, C. A., RUNKEL, A. C., RUNNEGAR, B., STEWART, M. C. & PALMER, A. R. 2004. The Late Cambrian Spice (13C) Event and the Sauk II-SAUK III Regression: New Evidence from Laurentian Basins in Utah, Iowa, and Newfoundland. *Journal of Sedimentary Research* **74**(3), 366-77.

SALTZMAN, M. R., RIPPERDAN, R. L., BRASIER, M., LOHMANN, K. C., ROBISON, R. A., CHANG, W., PENG, S., ERGALIEV, E. & RUNNEGAR, B. 2000. A global carbon isotope excursion (SPICE) during the Late Cambrian: relation to trilobite extinctions, organic-matter burial and sea level. *Palaeogeography, Palaeoclimatology, Palaeoecology* **162**(3), 211-23.

SATO, T., ISOZAKI, Y., HITACHI, T. & SHU, D. 2014. A unique condition for early diversification of small shelly fossils in the lowermost Cambrian in Chengjiang, South China: Enrichment of phosphorus in restricted embayments. *Gondwana Research* **25**(3), 1139-52.

SKOVSTED, C. B., BROCK, G. A. & PATERSON, J. R. 2006. Bivalved arthropods from the Lower Cambrian Mernmerna Formation, Arrowie Basin, South Australia and their implications for identification of Cambrian 'small shelly fossils'. *Memoirs of the Association of Australasian Palaeontologists* **32**, 7-41.

SKOVSTED, C. B., BROCK, G. A., LINDSTRÖM, A., PEEL, J. S., PATERSON, J. R. & FULLER, M. K. 2007. Early Cambrian record of failed durophagy and shell repair in an epibenthic mollusc. *Biology Letters* **3**(3), 314-17.

SKOVSTED, C. B., BROCK, G. A., PATERSON, J. R., HOLMER, L. E. & BUDD, G. E. 2008. The scleritome of Eccentrotheca from the Lower Cambrian of South Australia: Lophophorate affinities and implications for tommotiid phylogeny. *Geology* **36**(2), 171-74.

SKOVSTED, C. B., BALTHASAR, U., BROCK, G. A. & PATERSON, J. R. 2009. The tommotiid Camenella reticulosa from the early Cambrian of South Australia: morphology, scleritome reconstruction, and phylogeny. *Acta Palaeontologica Polonica* **54**(3), 525-40.

SKOVSTED, C. B., BROCK, G. A. & TOPPER, T. P. 2011*a*. Sclerite fusion in the problematic early Cambrian spine-like fossil Stoibostrombus from South Australia. *Bulletin of Geosciences* **86**, 651-58.

SKOVSTED, C. B., BROCK, G. A., TOPPER, T. P., PATERSON, J. R. & HOLMER, L. E. 2011*b*. Scleritome construction, biofacies, biostratigraphy and systematics of the tommotiid Eccentrotheca helenia sp. nov. from the early Cambrian of South Australia. *Palaeontology* **54**(2), 253-86.

SKOVSTED, C. B., BROCK, G. A. & TOPPER, T. P. 2012. First occurrence of a new Ocruranus-like helcionelloid mollusc from the lower Cambrian of East Gondwana. *Gondwana Research* **22**(1), 256-61.

SKOVSTED, C. B., TOPPER, T. P., BETTS, M. J. & BROCK, G. A. 2014. Associated conchs and opercula of Triplicatella disdoma (Hyolitha) from the early Cambrian of South Australia. *Alcheringa: An Australasian Journal of Palaeontology* **38**(1), 148-53.

SKOVSTED, C. B., BETTS, M., TOPPER, T. & BROCK, G. 2015. The early Cambrian tommotiid genus Dailyatia from South Australia. *Memoir of the Association of Australasian Palaeontologists* **48**, 1-117.

SPRIGG, R. C. 1952. Sedimentation in the Adelaide Geosyncline and the formation of the continental terrace. In *Sir Douglas Mawson Anniversary Volume* (eds M. F. Glaessner and E. A. Rudd). pp. 153-59. University of Adelaide, Adelaide.

STEINER, M., LI, G., QIAN, Y. & ZHU, M. 2004. Lower Cambrian Small Shelly Fossils of northern Sichuan and southern Shaanxi (China), and their biostratigraphic importance. *Geobios* **37**(2), 259-75.

STEINER, M., LI, G., QIAN, Y., ZHU, M. & ERDTMANN, B.-D. 2007. Neoproterozoic to Early Cambrian small shelly fossil assemblages and a revised biostratigraphic correlation of the Yangtze Platform (China). *Palaeogeography, Palaeoclimatology, Palaeoecology* **254**(1-2), 67-99.

SWART, P. K. 2015. The geochemistry of carbonate diagenesis: The past, present and future. *Sedimentology* **62**(5), 1233-304.

TEPPER, J. G. O. 1879. Introduction to the cliffs and rocks at Ardrossan, Yorke's Peninsula. *Transactions of the Royal Society of South Australia* **2**, 71-79.

TOPPER, T. P., HOLMER, L. E., SKOVSTED, C. B., BROCK, G. A., BALTHASAR, U., LARSSON, C. M., STOLK, S. P. & HARPER, D. A. 2013. The oldest brachiopods from the lower Cambrian of South Australia. *Acta Palaeontologica Polonica* **58**(1), 93-109.

WEISSERT, H. & ERBA, E. 2004. Volcanism, CO2 and palaeoclimate: a Late Jurassic–Early Cretaceous carbon and oxygen isotope record. *Journal of the Geological Society* **161**(4), 695-702.

WEISSERT, H., JOACHIMSKI, M. & SARNTHEIN, M. 2008. Chemostratigraphy. *Newsletters on Stratigraphy* **42**(3), 145-79.

WENDLER, I. 2013. A critical evaluation of carbon isotope stratigraphy and biostratigraphic implications for Late Cretaceous global correlation. *Earth-Science Reviews* **126**, 116-46.

ZANG, W.-l., MOCZYDLOWSKA, M. & JAGO, J. B. 2007. Early Cambrian acritarch assemblage zones in South Australia and global correlation. *Australasian Palaeontological Memoirs* **33**, 141-70.

ZHOU, B. & XIAO, L. 1984. Early Cambrian monoplacophorans and gastropods from Huainan and Huoqiu counties, Anhui Province. *Professional Papers of Stratigraphy and Palaeontology* **13**, 125-40.

ZHOU, C., ZHANG, J., LI, G. & YU, Z. 1997. Carbon and oxygen isotopic record of the Early Cambrian from the Xiaotan Section, Yunnan, South China. *Scientia geologica sinica* **32**(2), 201-11.

ZHU, M.-Y., BABCOCK, L. E. & PENG, S.-C. 2006. Advances in Cambrian stratigraphy and paleontology: Integrating correlation techniques, paleobiology, taphonomy and paleoenvironmental reconstruction. *Palaeoworld* **15**(3-4), 217-22.

ZHU, M.-Y., ZHANG, J.-M., LI, G.-X. & YANG, A.-H. 2004. Evolution of C isotopes in the Cambrian of China: implications for Cambrian subdivision and trilobite mass extinctions. *Geobios* **37**(2), 287-301.

ZHURAVLEV, A. Y. & GRAVESTOCK, D. I. 1994. Archaeocyaths from Yorke Peninsula, South Australia and archaeocyathan Early Cambrian zonation. *Alcheringa: An Australasian Journal of Palaeontology* **18**(1-2), 1-54.

7. Supplementary material

Supplementary Table S1. Carbon- and oxygen-isotope ratios from WANG/1.0-195.0

Sample	**$\delta^{18}O$**	*SE*	**$\delta^{13}C$**	*SE*	**$\delta^{18}O$**	*SE*	**$\delta^{13}C$**	*SE*
1	**-9.75**	*0.27*	**2.33**	*0.16*				
1	**-9.43**	*0.27*	**2.26**	*0.13*				
12	**-9.57**	*0.27*	**3.70**	*0.13*				
12	**-9.84**	*0.31*	**3.60**	*0.11*				
20	**-11.49**	*0.25*	**2.36**	*0.18*				
20	**-11.52**	*0.28*	**2.41**	*0.15*				
30	**-9.89**	*0.28*	**2.26**	*0.11*				
40	**-10.65**	*0.33*	**2.93**	*0.11*				
40	**-11.08**	*0.29*	**2.88**	*0.15*				
50	**-11.13**	*0.25*	**3.17**	*0.19*				
60	**-9.97**	*0.31*	**1.81**	*0.15*				
60	**-9.44**	*0.26*	**2.03**	*0.14*				
70	**-8.66**	*0.29*	**4.45**	*0.15*	**-8.69**	*0.18*	**4.56**	*0.15*
80	**-8.00**	*0.29*	**-0.55**	*0.19*	**-7.97**	*0.15*	**-0.03**	*0.21*
90					**-10.32**	*1.95*	**-1.21**	*0.76*
100					**-8.39**	*0.60*	**2.00**	*0.42*
110a	**-6.45**	*0.25*	**3.32**	*0.17*				
110	**-8.25**	*0.27*	**4.62**	*0.19*				
110	**-7.67**	*0.24*	**4.67**	*0.18*				
120	**-6.53**	*0.37*	**5.70**	*0.23*				
130	**-6.70**	*0.34*	**4.23**	*0.15*				
130	**-7.05**	*0.23*	**3.90**	*0.13*				
132	**-6.13**	*0.25*	**4.37**	*0.17*				
132	**-6.73**	*0.28*	**4.19**	*0.11*				
143			**1.98**	*0.18*	**-8.47**	*0.15*	**1.96**	*0.20*
143	**-8.36**	*0.45*	**1.79**	*0.18*				
146.5	**-3.72**	*0.27*	**-9.66**	*0.16*	**-4.85**	*0.11*	**-9.67**	*0.21*
152					**-5.44**	*0.25*	**-1.22**	*0.25*
167			**-1.39**	*0.14*	**-11.99**	*0.13*	**-1.37**	*0.20*
167	**-11.68**	*0.30*	**-1.52**	*0.11*				
176	**-10.23**	*0.53*	**-1.58**	*0.11*				
184	**-10.81**	*0.33*	**-1.91**	*0.13*				
184	**-10.85**	*0.30*	**-2.05**	*0.14*				
190	**-10.64**	*0.29*	**-3.02**	*0.13*				
195	**-9.00**	*0.81*	**-4.26**	*0.33*				

SE = standard error. Right-hand data are re-runs for uncharacteristic or missing data. Double sample numbers are repeats. Isotope values in bold, SE in italics.

Supplementary Table S2. Carbon- and oxygen-isotope ratios from WANG/200.0-404.0

Sample	$\delta^{18}O$	*SE*	$\delta^{13}C$	*SE*	$\delta^{18}O$	*SE*	$\delta^{13}C$	*SE*
200	**-9.24**	*0.48*	**-4.23**	*0.17*				
210	**-10.11**	*0.51*	**-2.99**	*0.14*				
215	**-6.28**	*0.45*	**-7.43**	*0.22*				
215	**-5.85**	*1.12*	**-7.14**	*0.27*				
225	**-6.90**	*0.23*	**-6.78**	*0.14*				
225	**-7.23**	*0.26*	**-6.88**	*0.15*				
230	**-9.52**	*0.27*	**-2.49**	*0.14*				
235	**-10.22**	*0.54*	**-3.27**	*0.22*				
251	**-10.92**	*0.54*	**-3.05**	*0.24*				
256	**-11.57**	*0.57*	**-2.97**	*0.17*				
256	**-11.27**	*0.60*	**-3.06**	*0.30*				
260	**-11.36**	*0.29*	**-2.77**	*0.11*				
270	**-11.41**	*0.58*	**-3.29**	*0.20*				
283	**-9.90**	*0.34*	**-4.96**	*0.12*				
296	**-6.34**	*0.25*	**-6.79**	*0.11*	**-5.70**	*0.20*	**-7.39**	*0.16*
307	**-9.22**	*0.24*	**-2.68**	*0.12*				
307	**-9.31**	*0.21*	**-2.74**	*0.12*				
321	**-5.90**	*0.25*	**-7.29**	*0.11*	**-6.17**	*0.21*	**-6.55**	*0.23*
331	**-8.92**	*0.27*	**-1.96**	*0.15*				
331	**-8.82**	*0.30*	**-2.05**	*0.14*				
342	**-9.28**	*0.26*	**-2.12**	*0.12*				
350	**-8.95**	*0.34*	**-1.94**	*0.15*				
350	**-9.06**	*0.24*	**-2.00**	*0.14*				
358	**-9.06**	*0.24*	**-2.10**	*0.11*				
358	**-9.06**	*0.30*	**-2.19**	*0.11*				
366	**-7.42**	*0.24*	**-2.30**	*0.13*				
372	**-8.40**	*0.26*	**-2.29**	*0.14*				
372	**-8.41**	*0.27*	**-2.42**	*0.15*				
380	**-7.89**	*0.27*	**-1.14**	*0.17*				
388	**-7.77**	*0.24*	**-1.37**	*0.11*	**-8.30**	*0.14*	**-0.96**	*0.20*
388			**-1.36**	*0.13*				
393	**-7.92**	*0.25*	**0.21**	*0.14*				
404	**-7.71**	*0.27*	**-0.02**	*0.14*				
404	**-6.34**	*0.23*	**0.00**	*0.13*				

SE = standard error. Right-hand data are re-runs for uncharacteristic or missing data. Double sample numbers are repeats. Isotope values in bold, SE in italics.